Supporting Information

New Near-infrared Rhodamine Dyes with Large Stokes Shifts for Sensitive Sensing of Cellular pH changes and Fluctuations

Yibin Zhang,[a,b] Shuai Xia,[a] Mingxi Fang,[a] Wafa Mazi,[a] Yanbo Zeng,[a] Taylor Johnston,[a] Adam Pap,[a] Rudy L. Luck[a*] and Haiying Liu[a*]

[a]Department of Chemistry, Michigan Technological University, Houghton, MI 49931, E-mail: hyliu@mtu.edu; rluck@mtu.edu

[b]School of Chemistry and Chemical Engineering, Yangtze Normal University, Chongqing 408100, China

CONTENTS

1. Summary of near-infrared fluorescent probes for detection of pH

Probe structure	Molar Absorption Coefficients (M^{-1} cm^{-1})	Absorbance Maxima (nm)	Emission Maxima (nm)	fluorescence Quantum Yields	solvent	pK_a	references
	3.3 x10^4	630	723	0.01	phosphate buffer containing 0.1% DMSO	7.1	1
	1.3 x 10^5	608	672	0.17 at pH	phosphate buffer	7.2	2
	2.65 x 10^4	554	657	0.12 at pH 1.6	phosphate buffer	2.4	3
	-	580	650	0.24	40 mM BR buffer	5.04	4
	7.28 x 10^4	546	655	0.22 at pH 2.3	ethanol/ water (2/1, v/v)	4.40	5
	5.45 x 10^4	572	722	0.026 at pH 2.0	acetonitrile–buffer (v/v, 3 : 7) solution	3.93	6
	3.0 x 10^4	529	680	0.01 at pH 8.0	phosphate buffer	6.3	7
		681	708	0.16 at pH 5.0	phosphate buffer	5.0	8

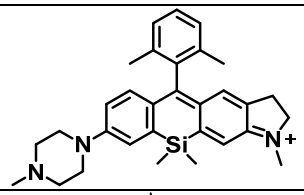	25000	605	683	0.18	phosphate buffer	6.1	9
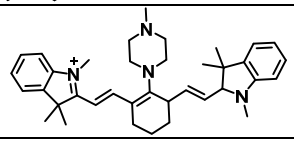	130000	759	789	0.03	phosphate buffer	5.5	10
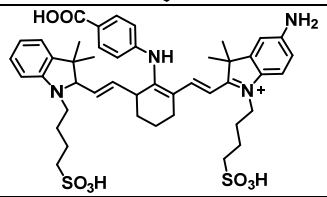		771	691	0.05	DMSO	4.71	11
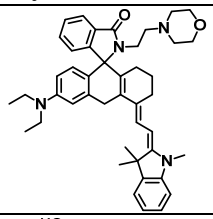		720	739	0.08	B-R buffer	4.98	12
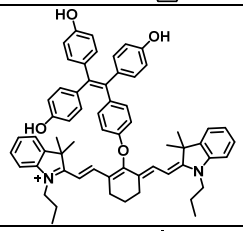		775	794	0.068	aqueous solution containing 30% ethanol	7.4	13
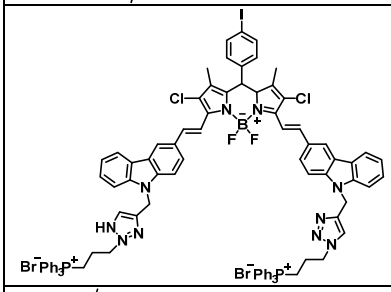	5.86×10^4	700	733	0.53	Ethanol	-	14
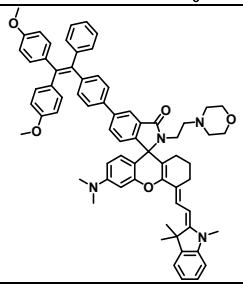	2.36×10^4	715	737	0.068 at pH 2.5	Citrate buffer containing 30% ethanol	4.9	15

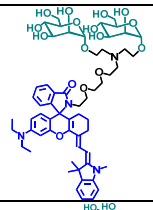	3.0 x 10^4	713	740	0.081 at pH 4.4	Citrate phosphate buffer containing 1% ethanol	6.1	[16]
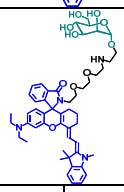	3.0 x 10^4	713	740	0.084 at pH 4.4	Citrate phosphate buffer containing 1% ethanol	5.8	[16]
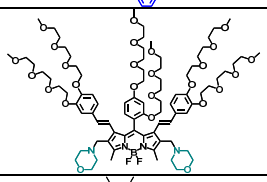		565	652	0.0032 at pH 7.4	Buffer with 1% DMSO	6.2	[17]
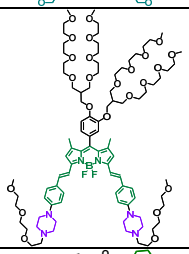	4.46 x 10^4 at pH 4.46	671	716	0.07 at pH 4.5	Buffer	3.57	[18]
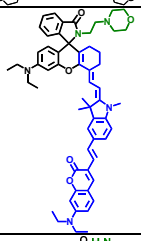	4.1×10^4 at pH 2.5	745	755	0.083 at pH 3.0	buffer containing 40% ethanol	4.2	[19]
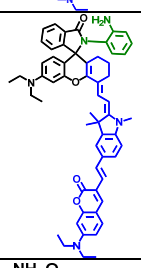	3.3×10^4 at pH 2.5	735	740	0.079 at pH 3.0	buffer containing 40% ethanol	4.8	[19]
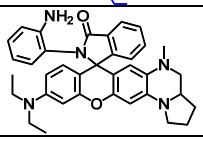	3.8×10^4 at pH 3.2	587	654	0.198 at pH 3.2	Buffer containing 10% ethanol	5.4	This work

2. Synthetic route to near-infrared rhodamine dyes A, B and C.

We showed how to prepare rhodamine dyes **A**-**C**, and characterize the products by NMR and Mass spectrometer.

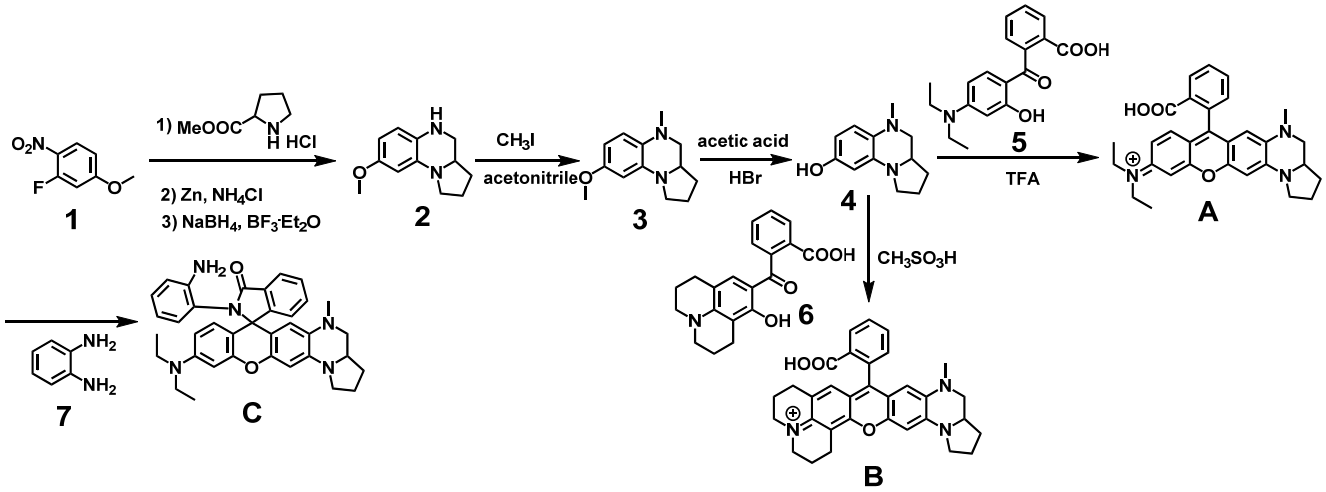

Scheme S1. Synthetic approach to prepare rhodamine dyes A-C.

Synthesis of rhodamine dye A: After compounds **4**[20] (204 mg, 1 mmol) and **5** (313 mg, 1 mmol) were added to trifluoroacetic acid (10 ml), the mixture was heated under reflux and stirred for 8 hours. When the reaction was cooled down to room temperature, the solvent was removed under reduced pressure. The resulting residue was purified by using flash column chromatography gradient elution with methanol ratio to dichloromethane from 0% to 10%. The rhodamines **A** was obtained as blue solid. ^{1}H NMR (400 MHz, CD_3OD) δ 8.30 (d, *J* = 7.7 Hz, 1H), 7.82 (t, *J* = 7.5 Hz, 1H), 7.75 (t, *J* = 7.5 Hz, 1H), 7.36 – 7.38 (m, 1H), 7.09 (d, *J* = 7.8 Hz, 1H), 6.97 (d, *J* = 9.3 Hz, 1H), 6.91 (s, 1H), 6.73 (s, 1H), 5.96 (d, *J* = 3.4 Hz, 1H), 3.57 – 3.74 (m, 4H), 2.77 – 2.91 (m, 2H), 2.67 (s, 3H), 2.22 – 2.26 (m, 3H), 2.02 – 2.07 (m, 2H), 1.56 – 1.59 (m, 2H), 1.26 (t, *J* = 7.1 Hz, 6H).; ^{13}C NMR (100 MHz, $CDCl_3$) δ 171.02, 160.32, 159.12, 157.60, 150.96, 139.80, 138.66, 135.10, 134.17, 133.60, 119.25, 117.17, 106.78, 98.50, 62.26, 56.65, 49.21, 42.21, 33.70, 26.74, 15.65. LCMS(ESI): calculated for $C_{30}H_{32}N_3O_3$ $[M]^+$482.2, found 482.5.

Synthesis of rhodamine dye B: Rhodamine **B** was prepared in the same way for synthesis of rhodamine **A** by using compounds **4**[20] (337 mg, 1 mmol) and **6**[21] (313 mg, 1 mmol), affording the product as blue solid. ^{1}H NMR (400 MHz, $CDCl_3$) δ: 8.18 (d, *J* = 7.4 Hz, 1H), 7.68 (q, *J* = 6.6 Hz, 2H), 7.32 – 7.23 (m, 1H), 6.72 (d, *J* = 6.5 Hz, 1H), 6.67 (s, 1H), 6.02 (d, *J* = 2.9 Hz, 1H), 3.71 – 3.84 (m, 2H), 3.45 – 3.55 (m, 4H), 3.08 – 2.96 (m, 2H), 2.62 – 2.69 (m, 7H), 2.27 – 2.16 (m, 2H), 2.06 (d, *J* = 5.9 Hz, 3H), 1.96 – 1.83 (m, 2H), 1.62 – 1.47 (m, 2H).; ^{13}C NMR (100 MHz, $CDCl_3$) δ: 155.92, 154.36, 151.61, 149.71, 145.91, 135.44, 134.25, 131.03, 130.50, 129.97, 125.53, 123.79, 114.50, 104.74, 103.83, 94.28, 58.11, 52.60, 50.50, 47.66, 38.35, 29.84, 27.61, 22.90, 20.85, 19.96. LCMS(ESI): calculated for $C_{32}H_{32}N_3O_3$ $[M]^+$506.2, found 506.5.

Synthesis of rhodamine dye C: After 1,2-diaminobenzene (324 mg, 3 mmol), rhodamines **A** (482 mg, 1 mmol), BOP reagent (530 mg, 1.2 mmol) and triethylamine(2 mL) were added to dry DCM (15 ml), the mixture was stirred at room temperature for 16 hours. Then the mixture was diluted with DCM, washed with water and brine, dried with anhydrous Na_2SO_4, filtered and concentrated in vacuo. The resulting residue was purified by using flash column chromatography gradient elution with methanol ratio to dichloromethane from 0% to 5%. The rhodamines **C** was obtained as blue solid. ^{1}H NMR (400 MHz, $CDCl_3$) δ: 7.95 (d, *J* = 7.5, Hz, 1H), 7.67 – 7.56 (m, 2H), 7.24 – 7.16 (m, 1H), 6.89 (d, *J* = 7.7, 1H), 6.57 (d, *J* = 8.1, 2H), 6.42 – 6.16 (m, 3H), 6.04 – 5.89 (m, 2H), 5.78 (s, 1H), 3.74 – 3.65 (m, 1H), 3.32 (d, *J* = 5.3 Hz, 5H), 3.14 (s, 1H), 2.47 (s, 3H), 2.25 – 2.37 (m, 1H), 1.81 – 2.02 (m, 3H), 1.22 – 1.43 (m, 2H), 1.11 (t, *J* = 7.0 Hz, 6H).; ^{13}C NMR (100 MHz, $CDCl_3$) δ: 167.26, 154.33, 152.76, 149.06, 137.94, 133.04, 132.98, 131.82, 128.77, 128.69, 128.58, 128.35, 124.43, 122.76, 121.48, 117.28, 116.62, 107.97, 97.95, 96.64, 69.89, 57.03, 54.67, 47.46, 44.22, 38.93, 30.16, 23.53, 11.76. LCMS(ESI): calculated for $C_{36}H_{38}N_5O_2$ $[M]^+$572.3, found 572.5.

3. ^{1}H and ^{13}C NMR spectra of near-infrared rhodamine dyes A, B, and C.

In this section, we showed ^{1}H and 13C NMR spectra of probes A-C.

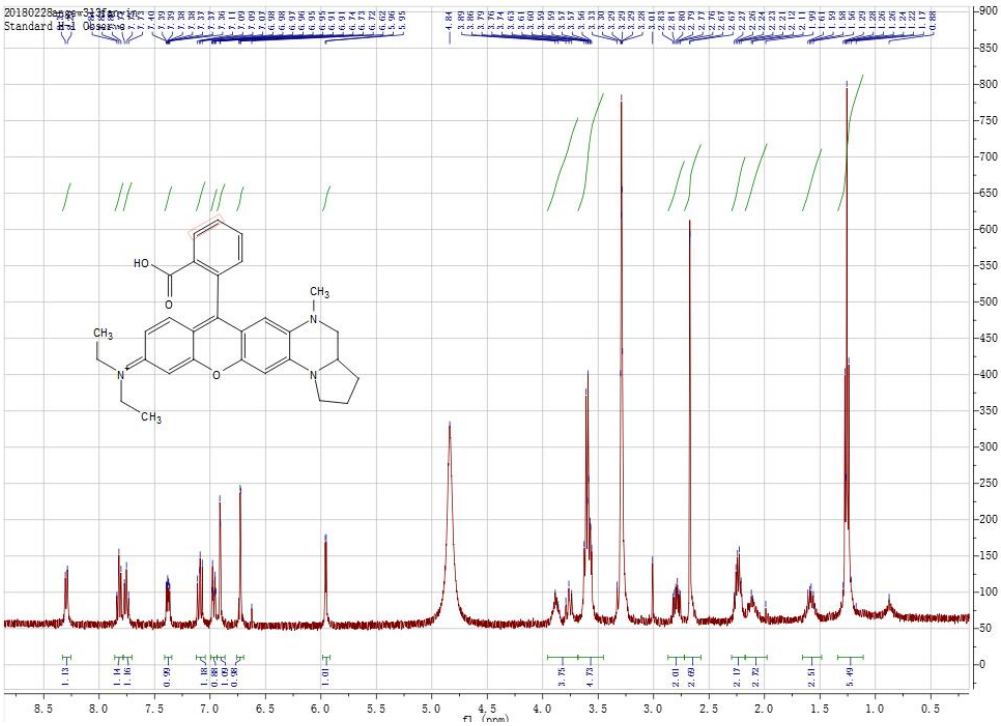

Figure S1. ^{1}H NMR spectrum of rhodamine dye **A** in CD_3OD solution.

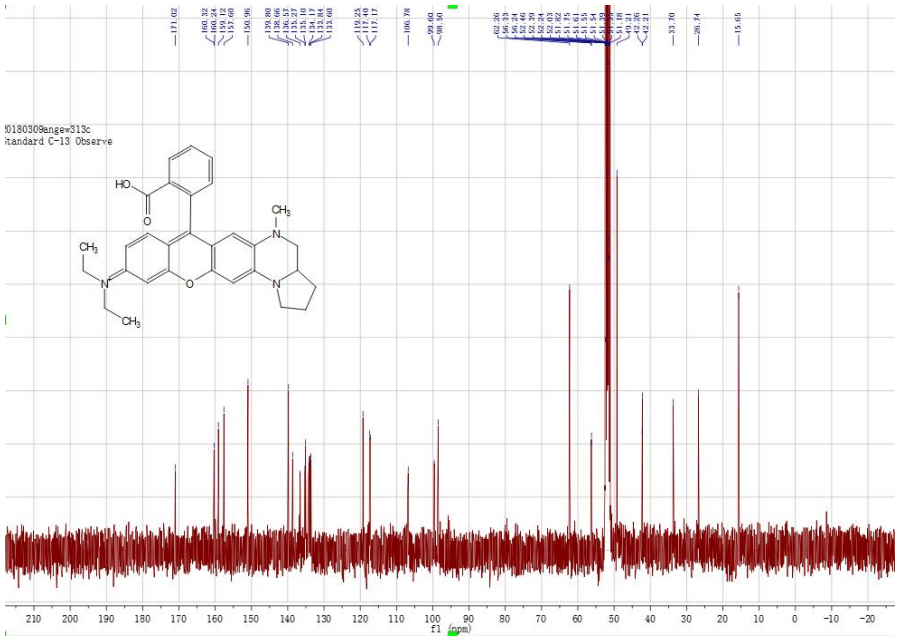

Figure S2. ^{13}C NMR spectrum of rhodamine dye **A** in CD_3OD solution.

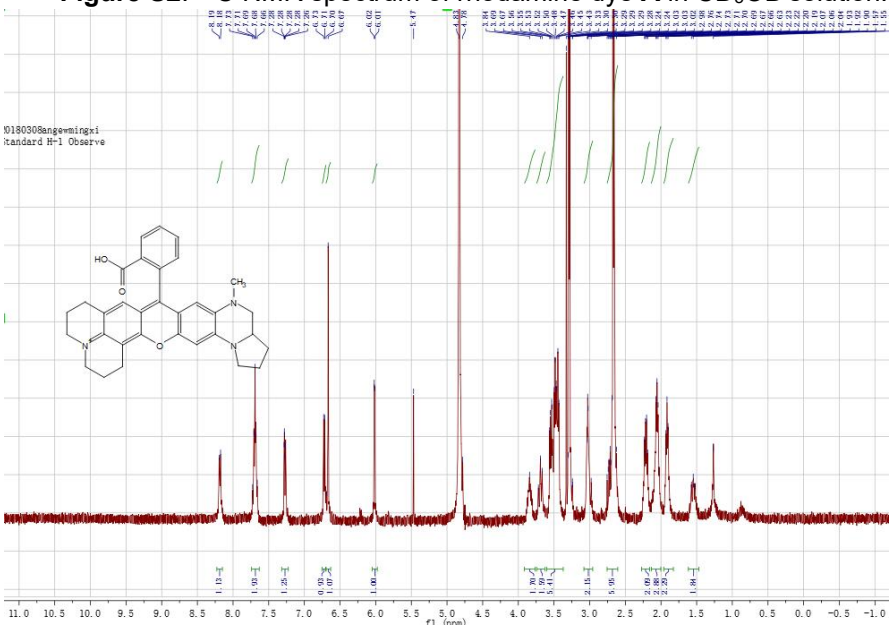

Figure S3. ^{1}H NMR spectrum of rhodamine dye **B** in CD_3OD solution.

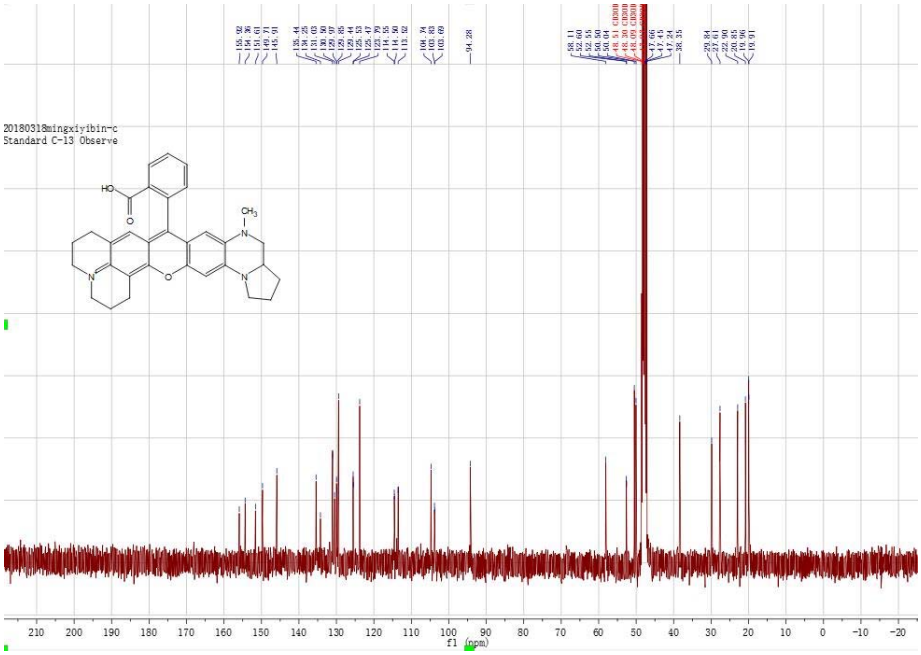

Figure S4. ^{13}C NMR spectrum of rhodamine dye **B** in CD_3OD solution.

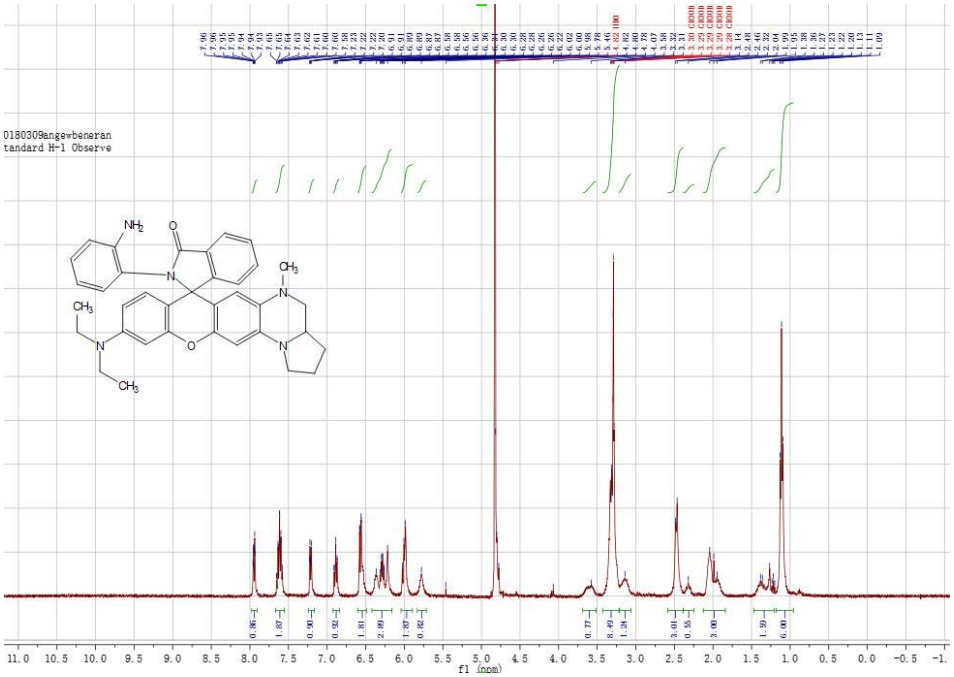

Figure S5. ^{1}H NMR spectrum of rhodamine dye **C** in CD_3OD solution.

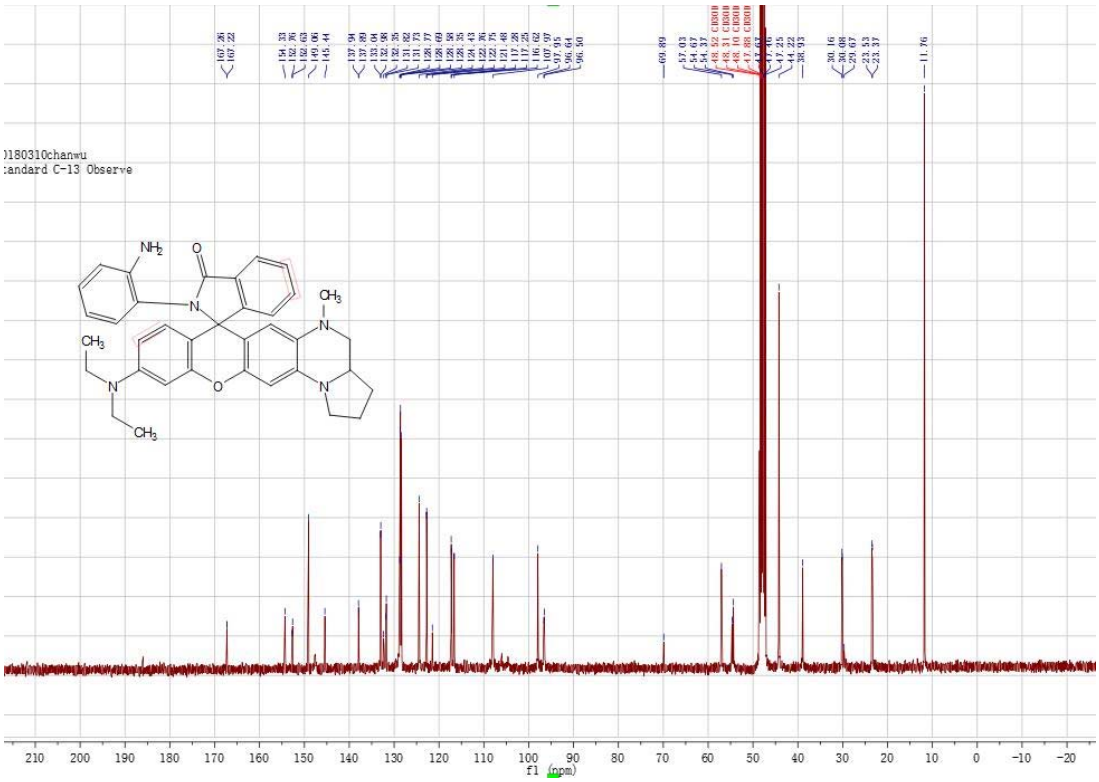

Figure S6. ^{13}C NMR spectrum of rhodamine dye **C** in CD_3OD solution.

4. A fluorescence standard and calculation of fluorescence quantum yields of the rhodamine dyes

We chose a near-infrared rhodamine dye shown below as a fluorescent standard to calculate fluorescence quantum yields of rhodamine dyes **A**, **B** and **C**.

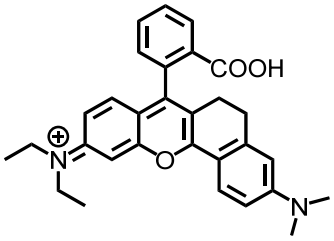

Near-infrared rhodamine dye as a fluorescence standard

The UV-Vis absorption spectra of rhodamine **A**, **B** and **C** were collected in the range from 300 to 800 nm with increments of 1 nm. For the buffers, we prepared citrate-phosphate buffer from pH 2.0 to pH 7.8, and carbonate-bicarbonate buffer for pH 8.8 to pH 11. Their corresponding fluorescence spectra were collected at the excitation wavelength of 550 nm with increments of 1 nm. The excitation and emission slit widths were set to 5 nm. A near-infrared rhodamine dye above[22, 23] was utilized as a reference standard to calculate the fluorescence quantum yields of rhodamine **A**, **B**, and **C** in ethanol and buffer solutions. The standard dye with a fluorescence quantum yield 37% in pH 7.4 PBS buffer with 10% ethanol was used. The absorbance was kept between 0.05 and 0.1 in order to obtain optimized data. All the samples and references were freshly prepared under identical conditions. The fluorescence quantum yields were calculated according to literature[4] using the equation below[24]:

$$\phi_X = \phi_{st}(Grad_X / Grad_{st})(\eta_X^2 / \eta_{st}^2)$$

Where Φ is the fluorescence quantum yield, the subscripts 'st' and 'X' stand for standard and test, respectively, "Grad" represents the gradient from the plot of integrated fluorescence intensity versus absorbance and η is the refractive index of the solvent.

We investigated effect of ethanol percentage in water-ethanol mixed solution on dye fluorescence intensity (Figure S7-S9). Increase of ethanol percentages from 1% to 60% causes the dye fluorescence intensity increases to reduce dye aggregation in aqueous solutions.

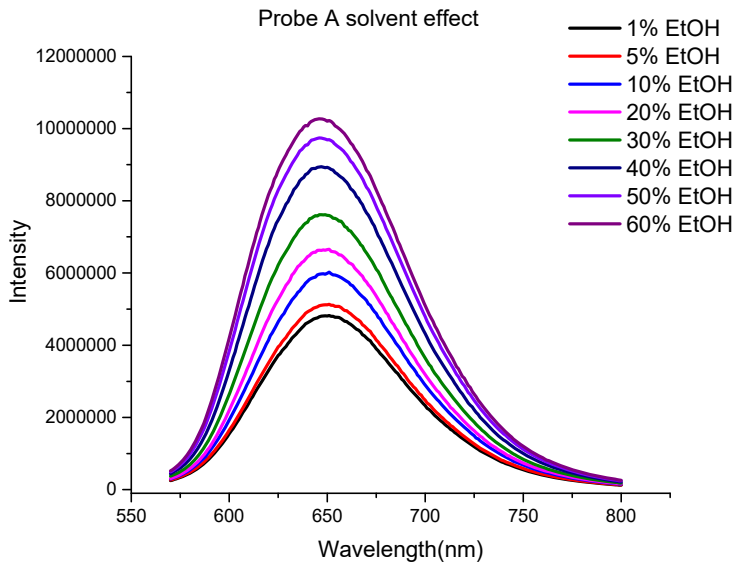

Figure S7. Fluorescence spectra of rhodamine dye **A** in 10 mM pH 7.4 buffers with different percentages of ethanol in ethanol and water mixed solution.

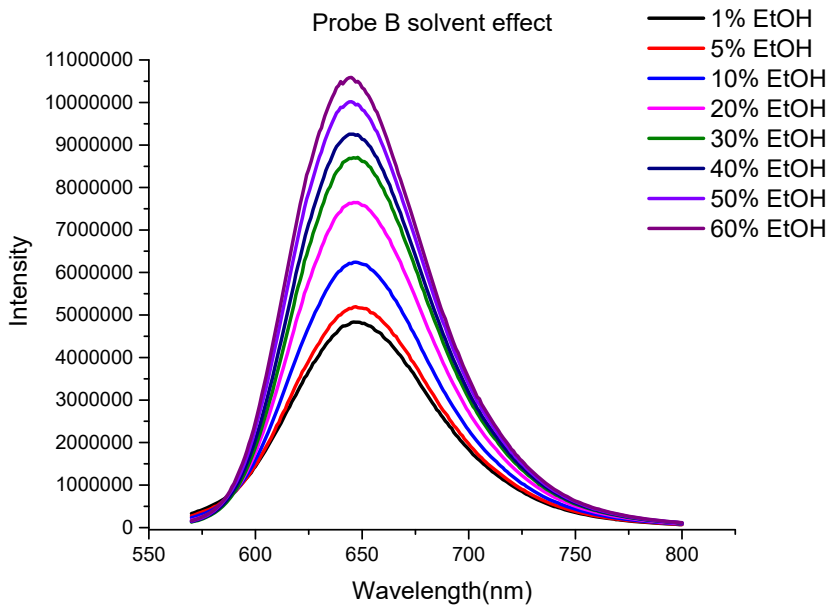

Figure S8. Fluorescence spectra of rhodamine dye **B** in 10 mM pH 7.4 buffers with different percentages of ethanol in ethanol and water mixed solution.

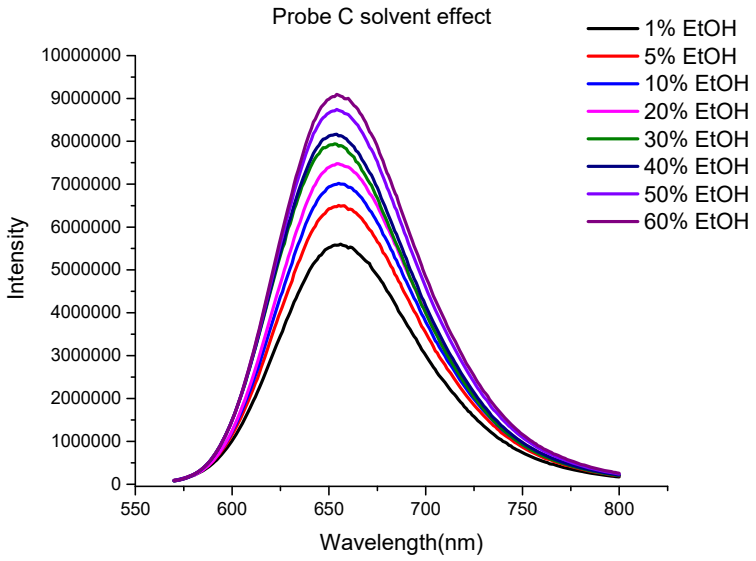

Figure S9. Fluorescence spectra of rhodamine dye **C** in 10 mM pH 2.4 buffers with different percentages of ethanol in ethanol and water mixed solution.

5. Determination of pK_a by fluorometric titration

pK_a of rhodamine dye **C** was obtained by using the equation below[25] through fluorometric titration as a function of pH, which was obtained by using the fluorescence spectra. The expression of the steady-state fluorescence intensity *F* as a function of the proton concentration has been extended for the case of n: 1 complex between H^+ and a fluorescent dye.

$$F = \frac{F_{\min}[H^+]^n + F_{\max}K_a}{K_a + [H^+]^n}$$

F_{min} and F_{max} stand for the fluorescence intensities at maximal and minimal H^+ concentrations, respectively while *n* is apparent stoichiometry of H^+ binding to the rhodamine dye C. Nonlinear fitting of equation expressed above to the fluorescence titration data was plotted as a function of H^+ concentration.

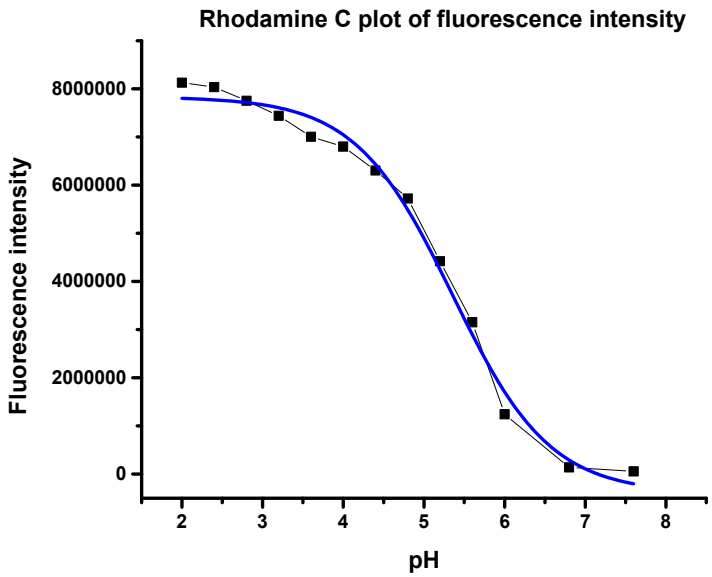

Figure S10. Plot curve of fluorescence intensity of rhodamine dye C versus pH

6. Dye stability and selectivity

We investigated fluorescence intensity of rhodamine dyes **A**, **B** and **C** under different excitation time, and study selectivity of rhodamine **C** to pH over different cations, anions, and amino acids. Rhodamine dyes **A**-**C** show excellent photo stability, and rhodamine **C** displays high selectivity to pH over cations, anions and amino acids.

Figure S11. Fluorescence intensity of rhodamine dyes **A** (left) and **B** (right) versus excitation time in 10 mM pH 5.0 buffers

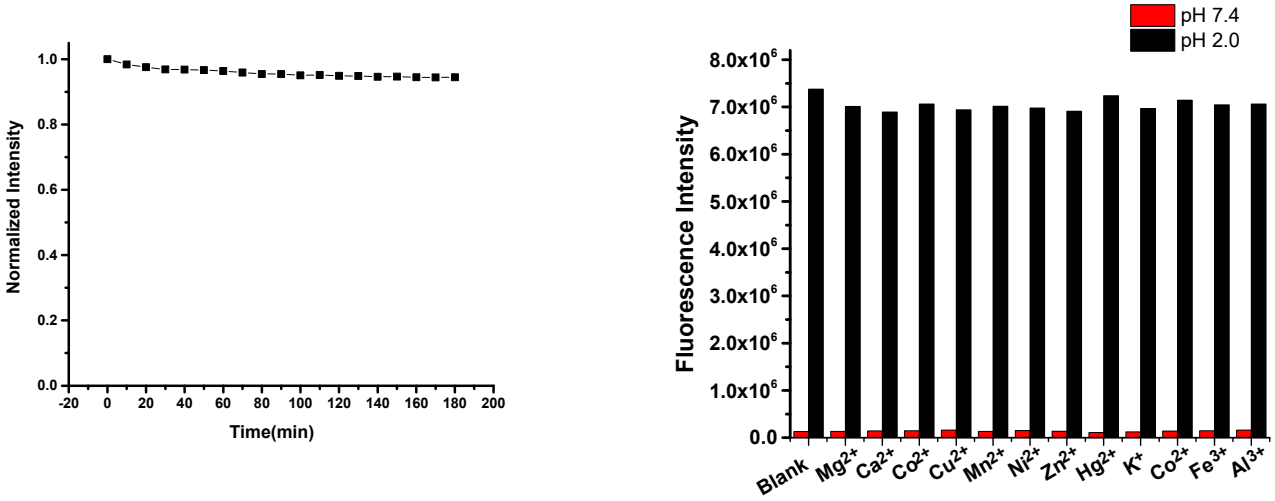

Figure S12. Fluorescence intensity of rhodamine dye **C** versus excitation time in 10 mM pH 2.0 buffer (left), and fluorescence responses (right) of rhodamine dye **C** to different metal ions in 10 mM buffers at pH 7,4 and 2.0 under excitation of 550 nm.

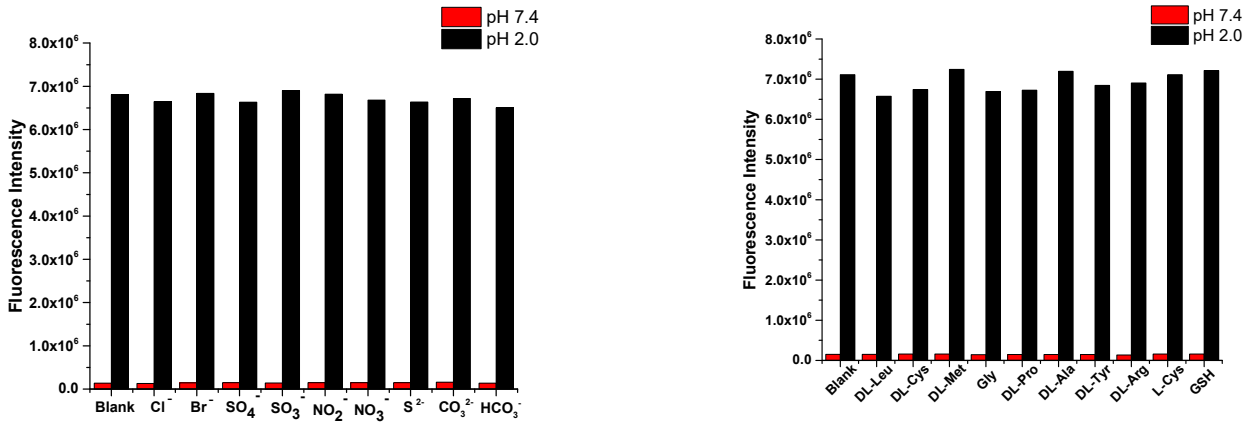

Figure S13. Fluorescence responses of rhodamine dye **C** to different anions and amino acids in 10 mM buffers at pH 7,4 and 2.0 under excitation of 550 nm.

7. Computationally derived structures for rhodamine dyes A-D.

The structures of rhodamine probes A-D were constructed using Avogadro[26, 27] and GaussView.[28] Structures were initially optimized using the capabilities within these aforementioned programs. Calculations were then conducted using density functional theory (DFT) with spherical atom dispersion terms, namely APFD,[29] with all electron basis sets at the 6-311+G(2d, p)[30-32] level implemented using the Gaussian16 suite of programs[33] for the full geometry optimization and frequency calculations of the probes. Imaginary frequencies were not obtained in any of the frequency calculations. The first six excited states were assessed on the basis of TD-DFT optimizations[34] in a Polarizable Continuum Model (PCM) of water.[35] Results were interpreted using Chemissian[36] for the UV-plots and GausView[28] for all other data and figures. The diagrams and listings of atomic positions from the calculations are listed sequentially for rhodamine dyes A-D below and all data are within the PCM matrix of water.

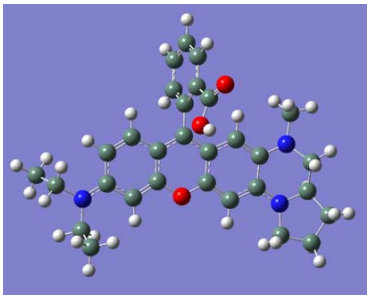

Figure S14. Drawing of rhodamine dye A with atoms represented as spheres of arbitrary size (H-white, C-grey, N-blue and O-red) using the GaussView[28] program.

Table S1. Atomic coordinates for rhodamine dye A.

Row	Symbol	X	Y	Z
1	C	2.9186	-1.43723	-0.31593
2	C	1.627969	-1.97698	-0.22453
3	C	0.532581	-1.14906	-0.24277
4	C	0.660267	0.258562	-0.33456
5	C	1.970222	0.794538	-0.40591
6	C	3.089058	0.002094	-0.40136
7	C	-0.50134	1.033538	-0.31166
8	C	-1.75166	0.405999	-0.2268
9	C	-1.81101	-1.00644	-0.16436
10	C	-2.99162	-1.70334	-0.07567
11	H	-2.93883	-2.78101	-0.01166
12	C	-4.21905	-1.01167	-0.03746
13	C	-4.17397	0.418345	-0.07861
14	C	-2.99116	1.086681	-0.16733
15	N	4.371741	0.500232	-0.48887
16	N	3.996547	-2.22124	-0.33075
17	C	-5.46609	-3.12009	-0.01831
18	C	-6.66708	-0.97413	0.183902
19	C	5.407718	-0.30638	0.134967
20	C	5.355802	-1.69853	-0.44251
21	C	6.179658	-2.76461	0.260388
22	O	-0.67735	-1.74405	-0.16973
23	C	4.551324	1.931599	-0.41117
24	H	5.628165	-1.65344	-1.50543
25	C	-0.41184	2.50711	-0.41402
26	C	0.091567	3.319675	0.61159
27	C	-0.78135	3.095913	-1.62116
28	C	0.224673	4.691458	0.405626
29	C	-0.65954	4.46529	-1.8117
30	H	-1.15595	2.465755	-2.42059
31	C	-0.15434	5.266983	-0.7959
32	C	0.511527	2.807088	1.941343
33	O	1.344485	3.347713	2.632377
34	O	-0.14253	1.702128	2.316864
35	H	0.209544	1.426127	3.176885
36	C	-7.28865	-0.59408	-1.15275
37	H	-8.25278	-0.10424	-0.99639
38	H	-6.64291	0.089628	-1.70869
39	H	-7.45427	-1.48012	-1.77067
40	H	2.071821	1.868971	-0.46185
41	H	1.476886	-3.04622	-0.16029
42	H	-2.99153	2.170122	-0.19892
43	H	-5.09163	0.989328	-0.05336
44	H	3.991592	2.427257	-1.20661
45	H	5.606896	2.160578	-0.55035
46	H	4.224802	2.343549	0.554111
47	C	3.98075	-3.66511	-0.1208
48	C	5.460254	-4.05129	-0.14631
49	H	6.125656	-2.61749	1.34403
50	H	7.228148	-2.74221	-0.03846
51	N	-5.39376	-1.6671	0.037769
52	H	-7.33168	-1.64392	0.734323
53	H	-6.53323	-0.09881	0.821374
54	H	-6.43092	-3.37591	-0.46193
55	H	5.28586	-0.34378	1.227718
56	H	6.377026	0.143106	-0.0819
57	H	5.671473	-4.8902	0.517067
58	H	5.75547	-4.34168	-1.1581
59	H	-0.95497	4.903802	-2.75882
60	H	-0.05601	6.3372	-0.93978
61	H	0.62142	5.298949	1.210812
62	H	3.515945	-3.88396	0.846699
63	H	3.398617	-4.16693	-0.89843
64	C	-5.32474	-3.77154	1.35089
65	H	-4.36092	-3.53297	1.806236
66	H	-6.11189	-3.42898	2.027122
67	H	-5.40223	-4.85783	1.262586
68	H	-4.70934	-3.49068	-0.71261

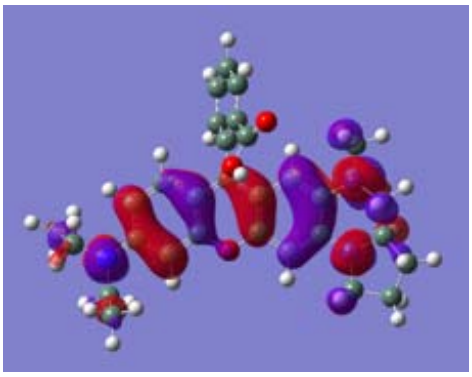

HOMO

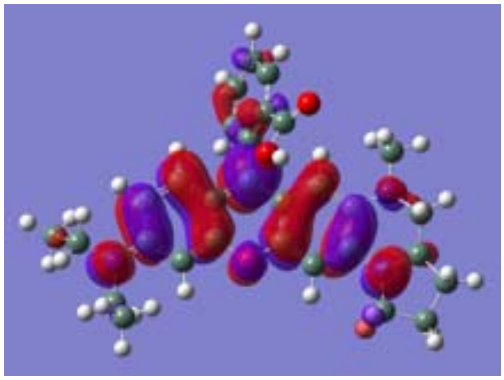

LUMO

Figure S15. The HOMO and LUMO for rhodamine dye **A**.

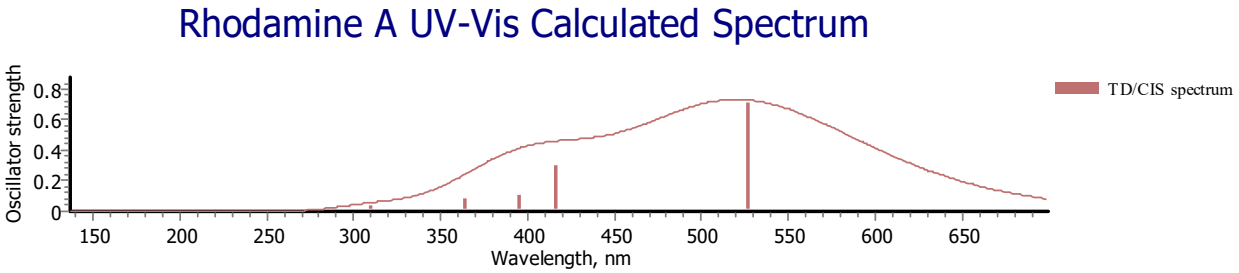

Energy[nm]	Oscillator Strength
526.3186	0.7013
416.0985	0.2919
394.9695	0.0981
363.4748	0.0816
318.7845	0.0118
309.9002	0.0366

Figure S16. Calculated UV-Vis spectrum for rhodamine dye **A** and listing of peak positions with oscillator strengths. This represents a HOMO-LUMO transition.

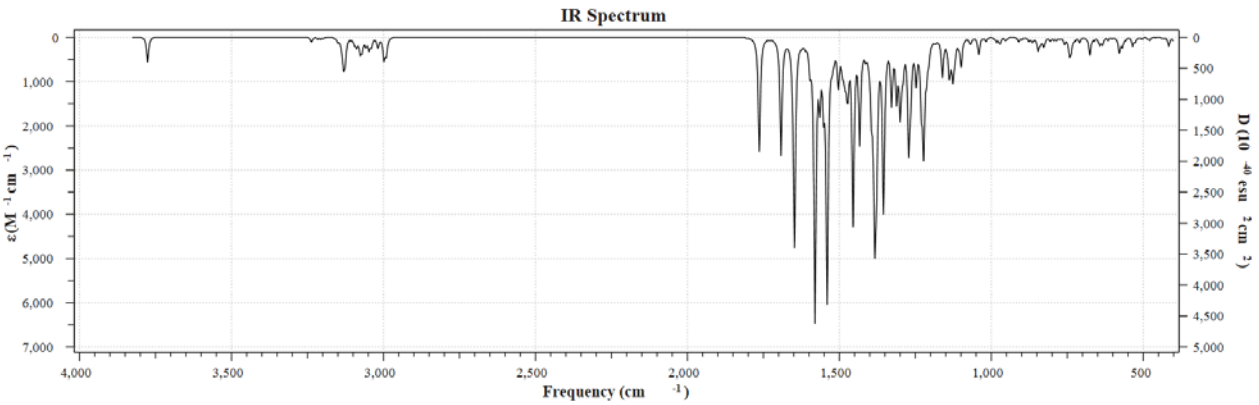

Figure S17. Calculated FTIR spectrum of rhodamine dye **A**.

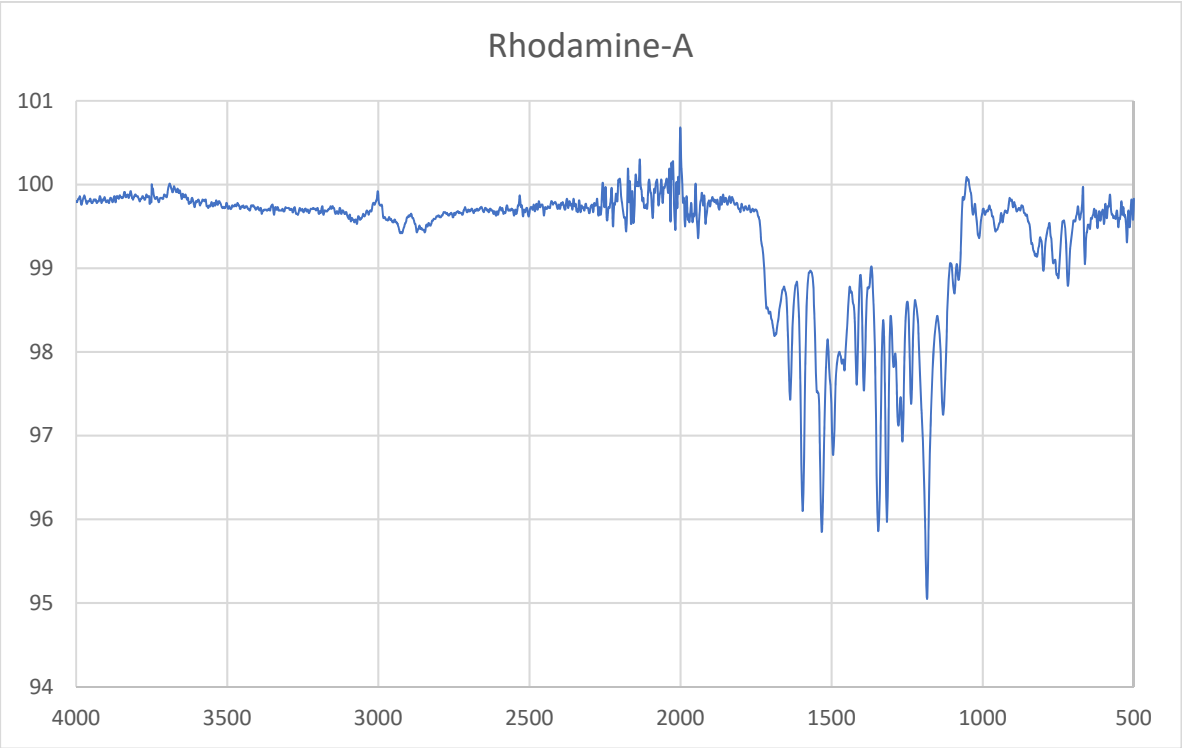

Figure S18. The solid state FTIR spectrum of rhodamine dye **A**.

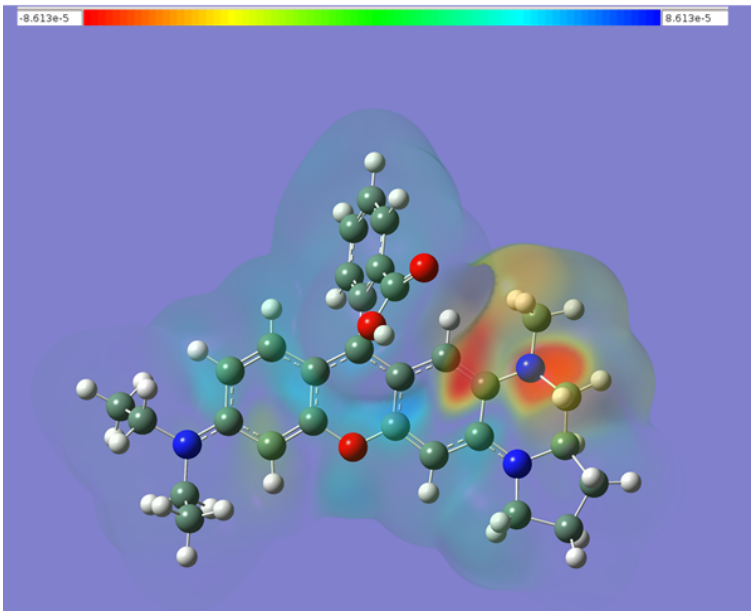

Figure S19. Current density difference plot for rhodamine dye **A** obtained by subtracting the SCF (ground state) density from the CI (excited state) density using the Cubegen program in GaussView.

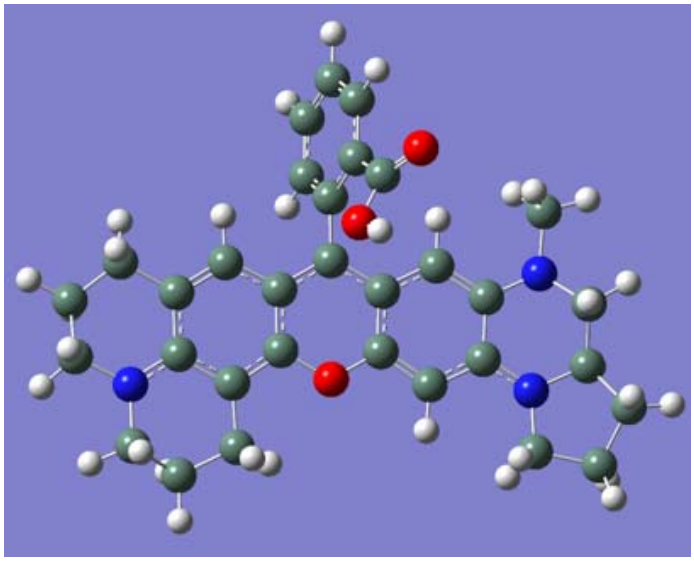

Figure S20. Drawing of rhodamine dye B with atoms represented as spheres of arbitrary size (H-white, C-grey, N-blue and O-red) using the GaussView[28] program.

Table S2. Atomic coordinates for rhodamine dye B.

Row	Symbol	X	Y	Z
1	C	3.106163	-1.29763	-0.26362
2	C	1.843912	-1.89282	-0.14255
3	C	0.70959	-1.11683	-0.17906
4	C	0.770031	0.288652	-0.31919
5	C	2.052011	0.882301	-0.42338
6	C	3.207119	0.142983	-0.40294
7	C	-0.43003	1.007281	-0.30985
8	C	-1.64694	0.326526	-0.19197
9	C	-1.64156	-1.08457	-0.08506
10	C	-2.7865	-1.84448	0.020606
11	C	-4.03243	-1.17526	0.052413
12	C	-4.07086	0.260066	-0.01203
13	C	-2.90963	0.959409	-0.14165
14	N	4.465047	0.698149	-0.52281
15	N	4.221965	-2.03071	-0.25781
16	C	-5.16632	-3.31311	0.386049
17	C	-4.01214	-3.97565	-0.33699
18	H	-4.01532	-5.04724	-0.1256
19	H	-4.14765	-3.85344	-1.4166
20	C	-2.70126	-3.34279	0.0994
21	C	5.540524	-0.03342	0.126084
22	C	5.553473	-1.44819	-0.39669
23	C	6.430156	-2.44418	0.344494
24	O	-0.46967	-1.76328	-0.07317
25	C	4.57586	2.138266	-0.49409
26	H	5.82192	-1.43099	-1.46157
27	C	-0.4103	2.479135	-0.46296
28	C	0.071658	3.348397	0.525805
29	C	-0.82566	3.010069	-1.68211
30	C	0.13793	4.717244	0.272478
31	C	-0.77075	4.376271	-1.91999
32	H	-1.18411	2.336587	-2.45307
33	C	-0.28685	5.234183	-0.94027
34	C	0.537478	2.901302	1.863856
35	O	1.360378	3.500078	2.518295
36	O	-0.06281	1.785167	2.29229
37	H	0.317098	1.55635	3.154362
38	C	-6.48255	-1.23361	0.262825
39	H	2.103311	1.957617	-0.51832
40	H	1.742742	-2.96501	-0.03991
41	H	-2.9489	2.042014	-0.19387
42	C	-5.38855	0.973902	0.087679
43	H	3.985707	2.579848	-1.29935
44	H	5.617908	2.41291	-0.65193
45	H	4.238666	2.566471	0.460538
46	C	4.275058	-3.46272	0.013006
47	C	5.771222	-3.77957	-0.00356
48	H	6.373499	-2.25488	1.421457
49	H	7.475365	-2.38481	0.039042
50	N	-5.18325	-1.87878	0.145272
51	H	-5.10504	-3.50365	1.466278
52	H	-6.12139	-3.71289	0.040571
53	H	5.424206	-0.03428	1.220241
54	H	6.486559	0.453265	-0.11272
55	H	6.024279	-4.57862	0.69359
56	H	6.076714	-4.09849	-1.00367
57	H	-1.10158	4.768613	-2.87567
58	H	-0.24043	6.302347	-1.12094
59	H	0.519374	5.369169	1.049848
60	H	3.823743	-3.663	0.991105
61	H	3.715734	-4.02523	-0.73969
62	H	-1.87553	-3.69938	-0.52042
63	H	-2.46358	-3.64466	1.127095
64	C	-6.51052	0.102074	-0.44959
65	H	-5.33251	1.927176	-0.44336
66	H	-5.59078	1.212107	1.139825
67	H	-7.48388	0.573416	-0.29616
68	H	-6.3856	-0.05477	-1.52624
69	H	-7.22097	-1.91572	-0.16424
70	H	-6.73518	-1.10662	1.324611

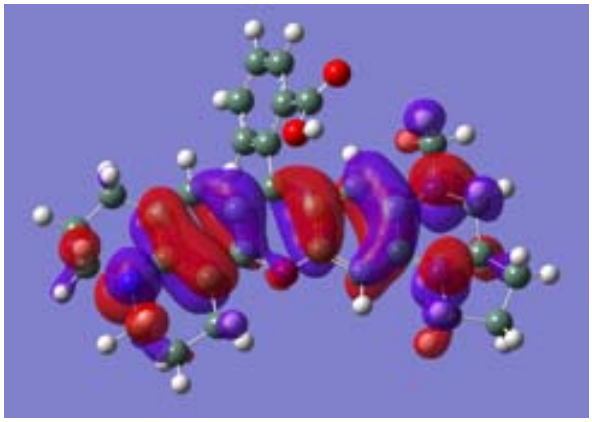

HOMO

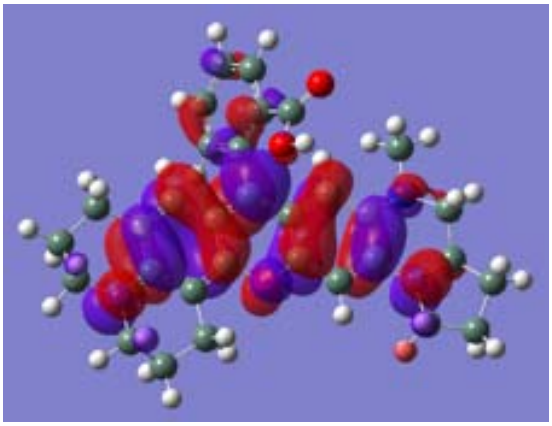

LUMO

Figure S21. The HOMO and LUMO for rhodamine dye **B**.

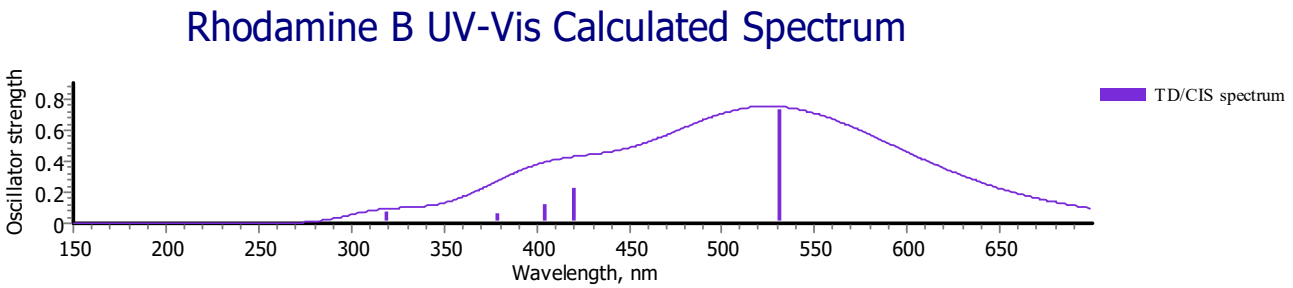

Energy[nm]	Oscillator Strength
530.6436	0.7265
420.0314	0.2276
403.8727	0.1180
378.6607	0.0533
325.7616	0.0227
319.0717	0.0652

Figure S22. Calculated UV-Vis spectrum for rhodamine dye **B** and listing of peak positions with oscillator strengths. This represents a HOMO-LUMO transition.

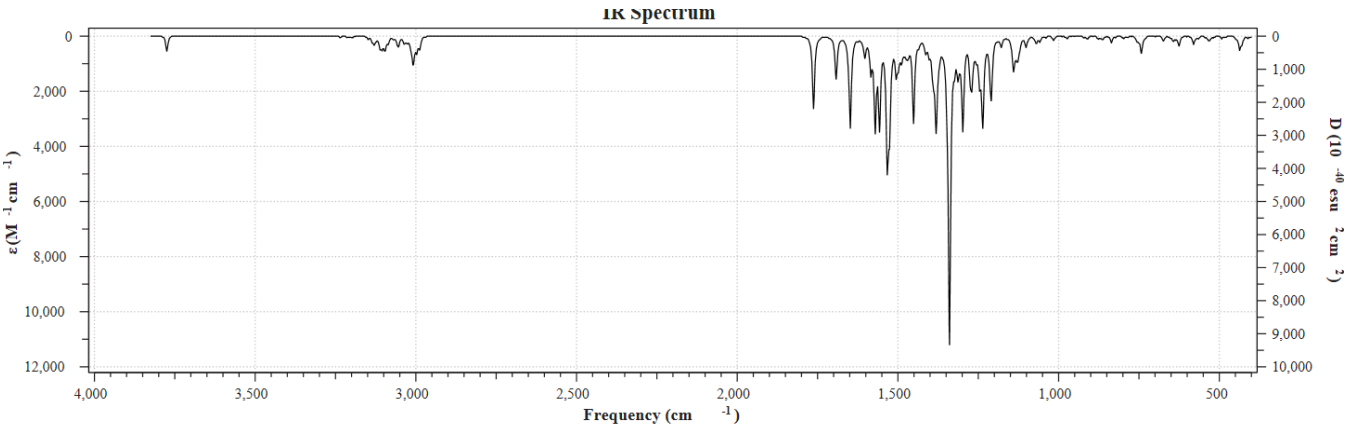

Figure S23. Calculated FTIR spectrum of rhodamine dye **B**.

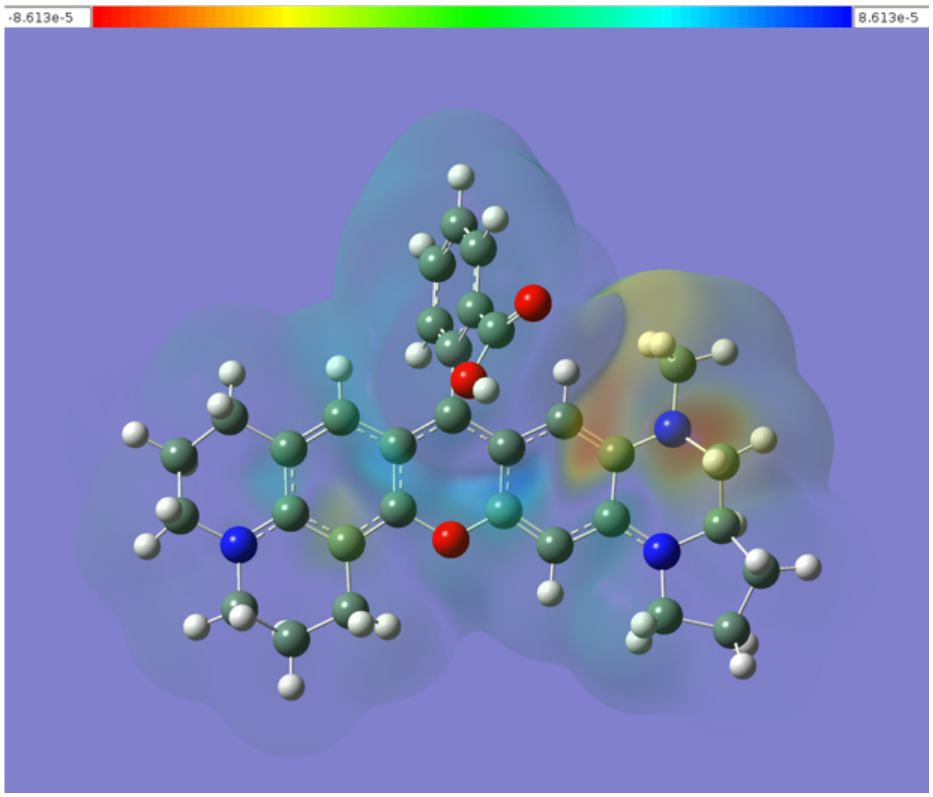

Figure S24. Current density difference plot for rhodamine dye B obtained by subtracting the SCF (ground state) density from the CI (excited state) density using the Cubegen program in GaussView.

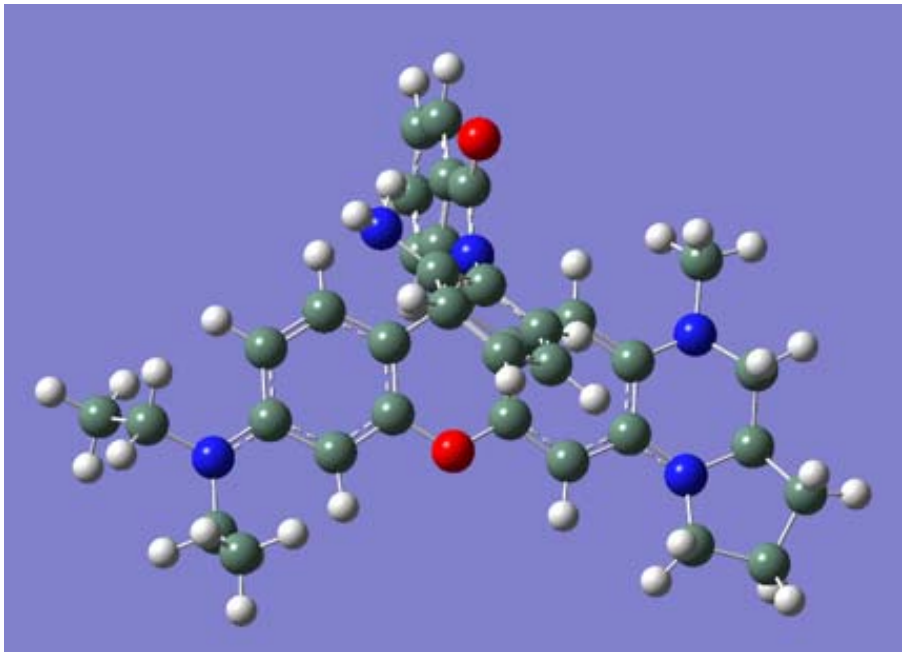

Figure S25. Drawing of rhodamine dye C with atoms represented as spheres of arbitrary size (H-white, C-grey, N-blue and O-red) using the GaussView[28] program.

Table S3. Atomic coordinates for rhodamine dye C.

Row	Symbol	X	Y	Z
1	C	3.284816	-1.22417	-0.7192
2	C	2.027323	-1.82252	-0.71884
3	C	0.872419	-1.05217	-0.63431
4	C	0.933231	0.324225	-0.54501
5	C	2.198981	0.924916	-0.52696
6	C	3.370976	0.200555	-0.6184
7	C	-0.29928	1.141932	-0.28719
8	C	-1.53141	0.321362	-0.54674
9	C	-1.47319	-1.06412	-0.64862
10	C	-2.61175	-1.84575	-0.78317
11	C	-3.88569	-1.25897	-0.83039
12	C	-3.94788	0.15374	-0.74668
13	C	-2.79961	0.898497	-0.60147
14	N	4.639399	0.787641	-0.61952
15	N	4.424509	-1.96102	-0.8261
16	C	-4.95353	-3.45249	-1.14283
17	C	-4.88168	-4.22596	0.169251
18	C	5.656324	-0.03537	0.01343
19	C	5.747923	-1.3575	-0.71504
20	C	6.565372	-2.43974	-0.02375
21	O	-0.30013	-1.76008	-0.61837
22	C	4.716403	2.192365	-0.29444
23	H	6.15106	-1.17046	-1.7203
24	C	-0.29141	2.446101	-1.04437
25	C	-0.32214	3.518865	-0.17284
26	C	-0.25199	2.646056	-2.41243
27	C	-0.3192	4.829759	-0.62511
28	C	-0.24864	3.956039	-2.88049
29	H	-0.22471	1.806205	-3.09892
30	C	-0.28157	5.039351	-1.9974
31	C	-0.36524	3.00944	1.212669
32	O	-0.45333	3.662524	2.251394
33	N	-0.31542	1.655195	1.127038
34	C	-6.34143	-1.43182	-0.87972
35	H	2.242044	2.000788	-0.40892
36	H	1.925196	-2.89781	-0.79606
37	H	4.133469	2.780268	-1.00605
38	H	5.755675	2.513167	-0.3672
39	H	4.350749	2.416286	0.719886
40	C	4.457084	-3.40087	-0.63364
41	C	5.949341	-3.7234	-0.57867
42	H	6.411011	-2.38127	1.059311
43	H	7.634636	-2.34873	-0.22206
44	N	-5.01635	-2.016	-0.95977
45	H	-5.84364	-3.75043	-1.70384
46	H	-4.10347	-3.69864	-1.7849
47	H	5.427557	-0.20882	1.077694
48	H	6.61472	0.48332	-0.0448
49	H	6.156575	-4.60275	0.03275
50	H	6.330536	-3.91839	-1.58549
51	H	-0.22004	4.142373	-3.94921
52	H	-0.27748	6.05017	-2.39124
53	H	-0.34581	5.657826	0.075204
54	H	3.950685	-3.66829	0.30453
55	H	3.945733	-3.92668	-1.44657
56	C	-6.87014	-0.94888	-2.22529
57	H	-7.01002	-2.19281	-0.46749
58	H	-6.33665	-0.61762	-0.15056
59	H	-6.91912	-1.77449	-2.94039
60	H	-6.22373	-0.1759	-2.64791
61	H	-7.87584	-0.53303	-2.11855
62	H	-5.75969	-4.02029	0.787447
63	H	-3.99422	-3.94825	0.742891
64	H	-4.84441	-5.30248	-0.01858
65	H	-2.47428	-2.9176	-0.83399
66	H	-4.8984	0.667019	-0.80328
67	H	-2.88251	1.978284	-0.52375
68	C	-0.43513	0.768777	2.222952
69	C	0.589556	-0.13773	2.48223
70	C	0.455105	-1.10444	3.467227
71	C	-0.71817	-1.14972	4.213669
72	C	-1.72553	-0.2252	3.993891
73	C	-1.60723	0.755431	3.001357
74	N	-2.63996	1.644998	2.757529
75	H	-2.62856	-0.25219	4.597308
76	H	1.258446	-1.80869	3.653239
77	H	-0.84436	-1.90065	4.987427
78	H	1.496469	-0.07916	1.892058
79	H	-2.33335	2.583324	2.534044
80	H	-3.34001	1.661749	3.485865

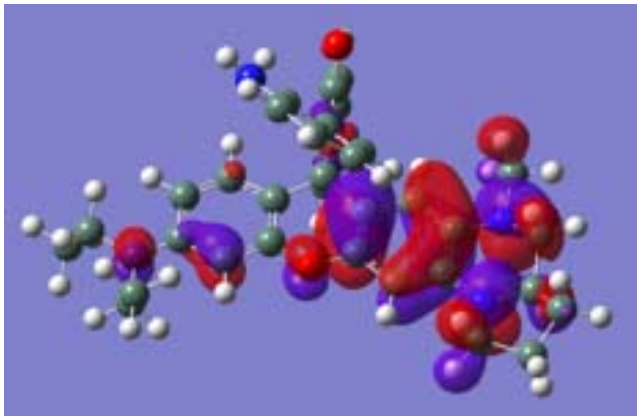

HOMO

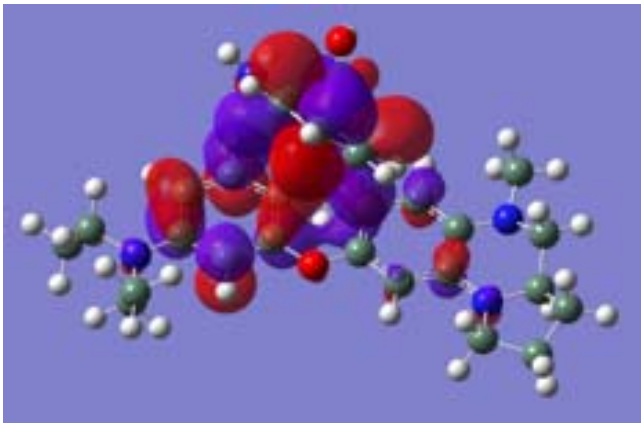

LUMO

Figure S26. The HOMO and LUMO+4 (see Fig. S31) for rhodamine dye **C**.

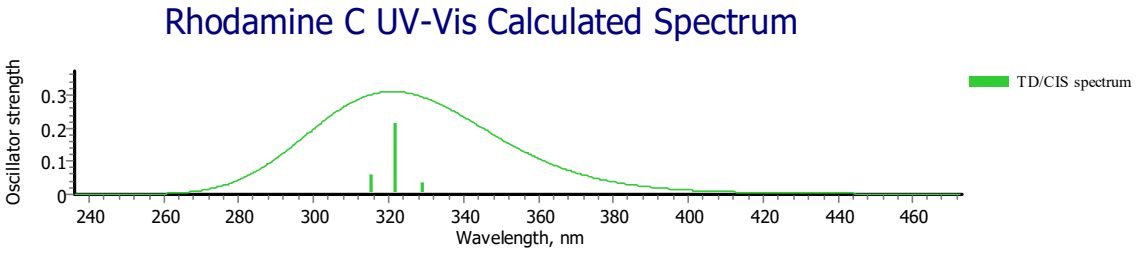

Energy[nm]	Oscillator Strength
400.2094	0.0038
358.5761	0.0014
328.9509	0.0354
321.7795	0.2127
315.2746	0.0568
309.0890	0.0100

Figure S27. Calculated UV-Vis spectrum for rhodamine dye C and listing of peak positions with oscillator strengths. This represents a HOMO-LUMO+4 transition.

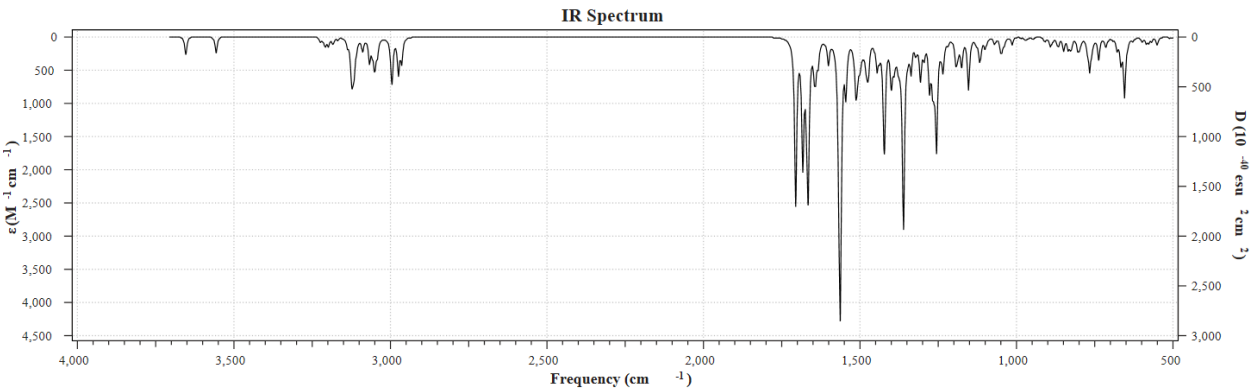

Figure S28. Calculated FTIR spectrum of rhodamine dye **C**.

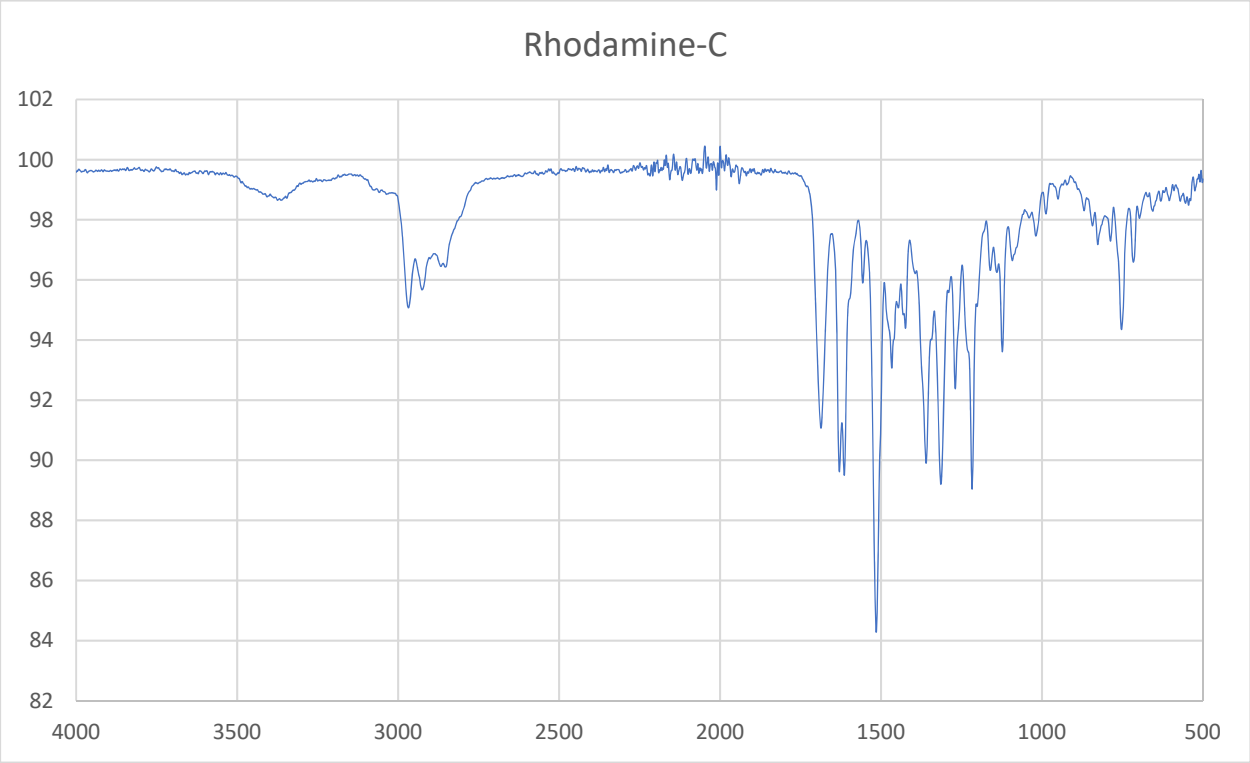

Figure S29. The solid state FTIR spectrum of rhodamine dye **C**.

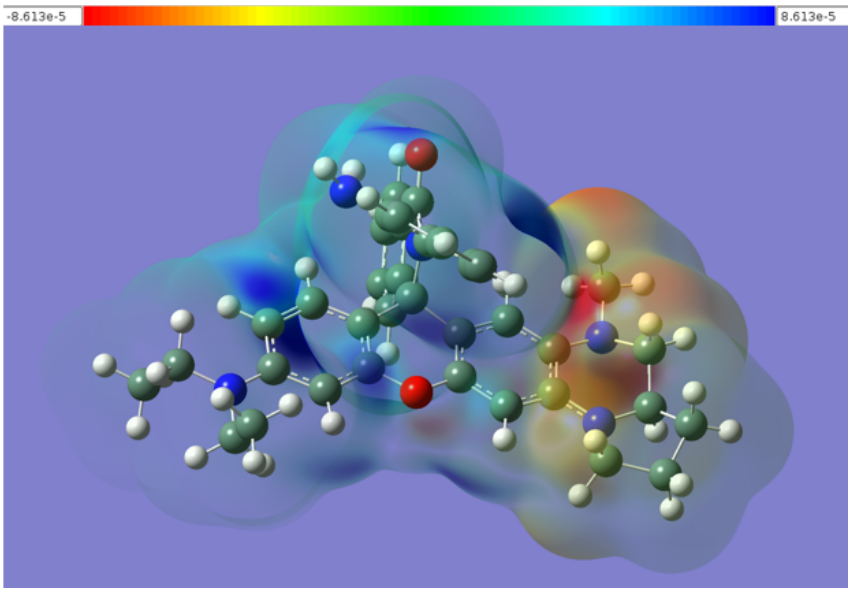

Figure S30. Current density difference plot for rhodamine dye **C** obtained by subtracting the SCF (ground state) density from the CI (excited state) density using the Cubegen program in GaussView.

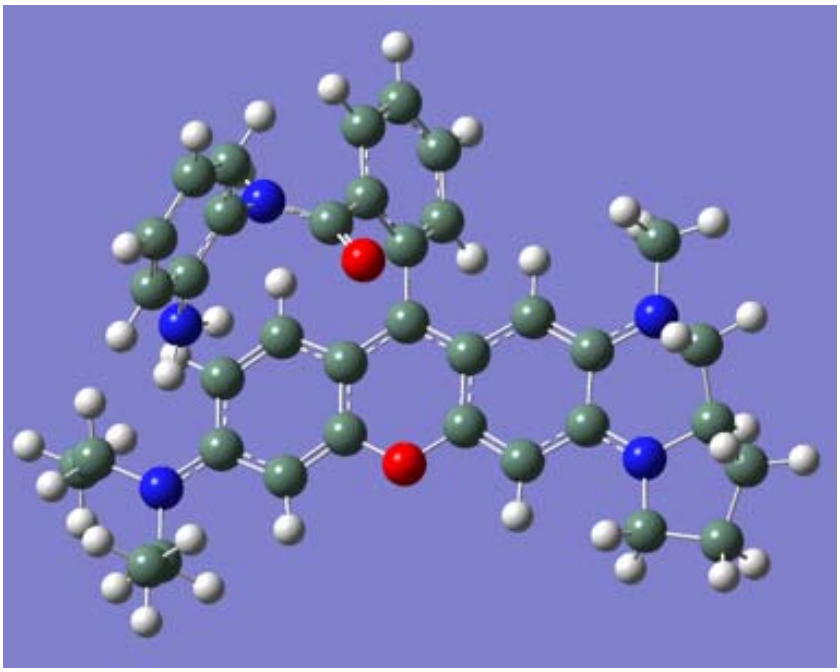

Figure S31. Drawing of rhodamine dye **D** with atoms represented as spheres of arbitrary size (H-white, C-grey, N-blue and O-red) using the GaussView[28] program.

Table S4. Atomic coordinates for rhodamine dye D.

Row	Symbol	X	Y	Z
1	C	-3.96667	1.075092	0.215158
2	C	-2.80188	1.853575	0.282925
3	C	-1.62549	1.376776	-0.23899
4	C	-1.5401	0.097209	-0.84356
5	C	-2.70804	-0.70503	-0.85088
6	C	-3.90706	-0.25753	-0.3601
7	C	-0.30448	-0.32198	-1.33263
8	C	0.798757	0.544237	-1.26034
9	C	0.655869	1.793089	-0.61482
10	C	1.704132	2.662022	-0.42649
11	C	2.987545	2.33611	-0.90889
12	C	3.127737	1.113096	-1.63822
13	C	2.078392	0.257274	-1.7912
14	N	-5.06594	-1.00407	-0.39017
15	N	-5.12934	1.530324	0.680485
16	C	3.91896	4.409849	0.002187
17	C	4.000209	4.256805	1.515546
18	C	-6.03392	-0.71849	0.655411
19	C	-6.36477	0.752505	0.62497
20	C	-7.15594	1.301403	1.800637
21	O	-0.54326	2.177318	-0.12289
22	C	-4.97654	-2.38278	-0.81143
23	H	-6.88125	0.982072	-0.31652
24	C	-0.1268	-1.67075	-1.90954
25	C	0.62739	-2.63739	-1.23197
26	C	-0.66299	-1.97031	-3.15682
27	C	0.829431	-3.88546	-1.81202
28	C	-0.45975	-3.22052	-3.72849
29	H	-1.23293	-1.2131	-3.68468
30	C	0.284917	-4.17931	-3.0558
31	C	1.129713	-2.34794	0.147618
32	O	0.404756	-1.83877	0.99249
33	N	2.42051	-2.68953	0.38187
34	C	5.400764	2.760896	-1.08488
35	H	-2.62483	-1.70365	-1.25587
36	H	-2.81696	2.837728	0.731649
37	H	-4.55305	-2.44451	-1.81565
38	H	-5.97966	-2.80576	-0.84244
39	H	-4.35873	-2.98963	-0.13445
40	C	-5.30506	2.785972	1.403323
41	C	-6.7879	2.785306	1.776552
42	H	-6.81071	0.832774	2.727992
43	H	-8.22643	1.119353	1.700565
44	N	4.048404	3.138825	-0.69547
45	H	4.721331	5.057011	-0.35853
46	H	2.987108	4.893219	-0.29779
47	H	-5.65153	-1.00101	1.647543
48	H	-6.93618	-1.29959	0.463025
49	H	-6.96638	3.288007	2.727262
50	H	-7.36913	3.303445	1.009172
51	H	-0.88428	-3.44236	-4.70165
52	H	0.438634	-5.1591	-3.49463
53	H	1.392036	-4.64275	-1.27566
54	H	-4.65976	2.786335	2.288538
55	H	-5.02541	3.638335	0.778494
56	C	5.750968	3.195146	-2.50102
57	H	6.079662	3.226836	-0.36717
58	H	5.527152	1.684423	-0.95706
59	H	5.658031	4.278615	-2.60946
60	H	5.091586	2.724901	-3.2343
61	H	6.780696	2.917077	-2.73835
62	H	4.955	3.813941	1.80973
63	H	3.200043	3.615265	1.891889
64	H	3.913955	5.231993	2.000594
65	H	1.512011	3.574462	0.120156
66	H	4.07886	0.851936	-2.08027
67	H	2.219713	-0.665	-2.34307
68	C	2.996937	-2.61643	1.682186
69	C	2.927693	-3.71784	2.523688
70	C	3.462163	-3.66947	3.803119
71	C	4.064594	-2.48997	4.233825
72	C	4.138474	-1.38612	3.401216
73	C	3.608341	-1.42625	2.104517
74	N	3.736871	-0.35155	1.251708
75	H	4.613536	-0.47283	3.747205
76	H	3.40511	-4.53363	4.455258
77	H	4.483002	-2.42823	5.233615
78	H	2.438781	-4.61547	2.158196
79	H	3.845418	0.550243	1.690932
80	H	3.106923	-0.3271	0.46332
81	H	2.969534	-3.0574	-0.38197

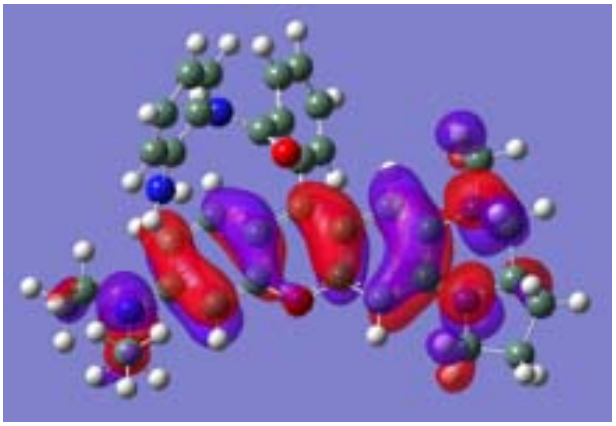

HOMO

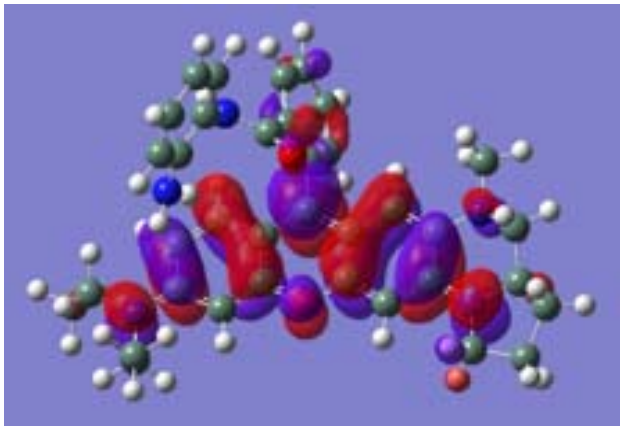

LUMO

Figure S32. The HOMO and LUMO for rhodamine dye **D**.

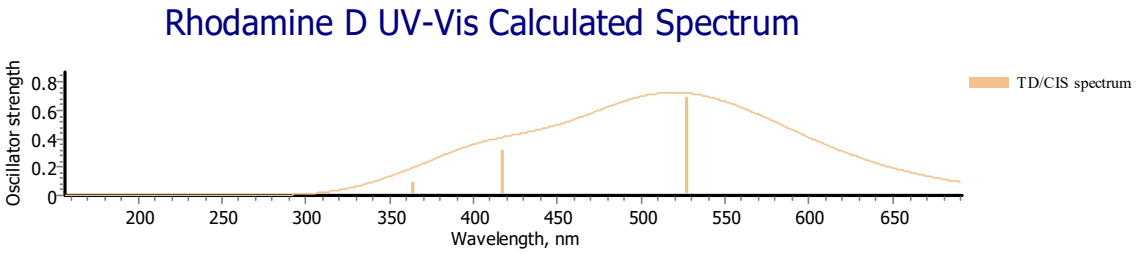

Energy[nm]	Oscillator Strength
526.8554	0.6902
454.2569	0.0059
417.6966	0.3179
363.9976	0.0905
351.2518	0.0095
321.0047	0.0102

Figure S33. Calculated UV-Vis spectrum for rhodamine dye **D** and listing of peak positions with oscillator strengths. This represents a HOMO-LUMO transition.

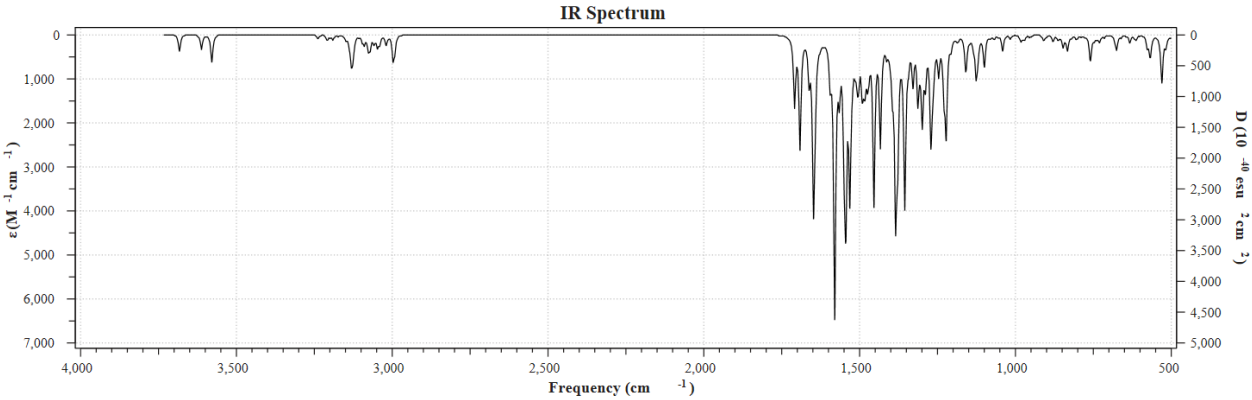

Figure S34. Calculated FTIR spectrum of rhodamine dye **D**.

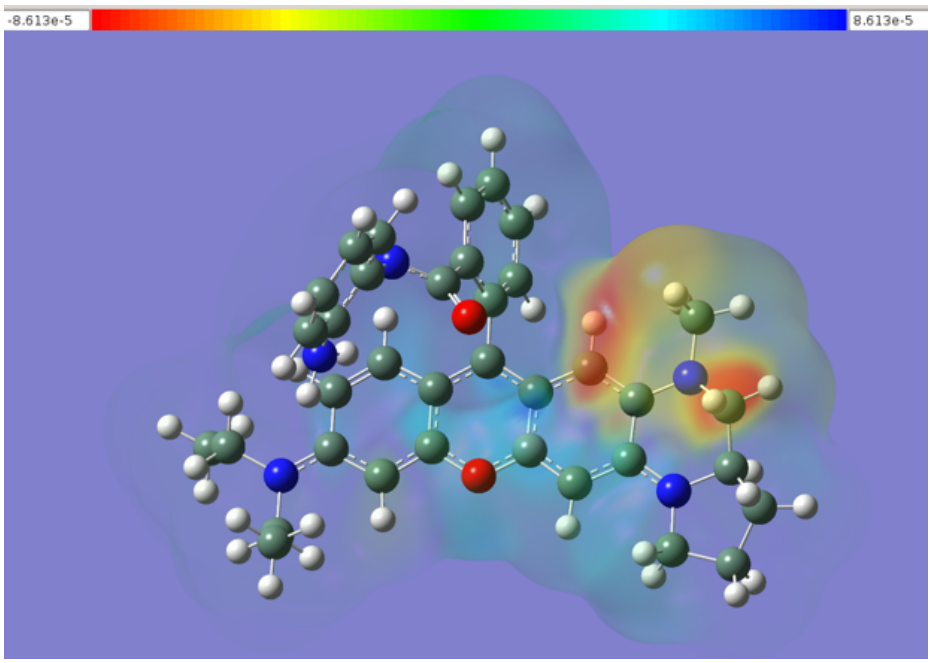

Figure S35. Current density difference plot for rhodamine dye **D** obtained by subtracting the SCF (ground state) density from the CI (excited state) density using the Cubegen program in GaussView.

8. Cytotoxicity of the rhodamine dyes

We used a standard MTS assay to investigate cytotoxicity of the rhodamine dyes A, B and C. The results show that the dyes have very low cytotoxicity.

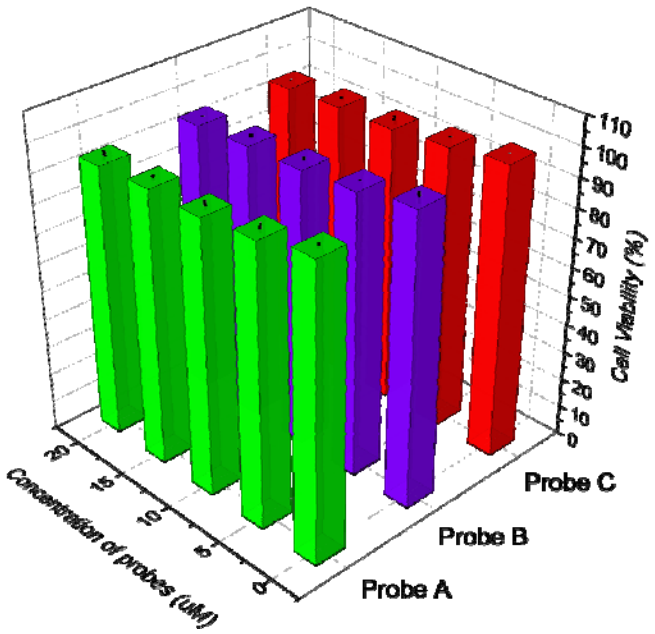

Figure S36. Cytotoxicity of rhodamine dyes **A**, **B**, and **C** through standard MTS assay by incubation of HeLa cells with 5, 10, 15, 20 μM of rhodamine dye **A**, **B**, or **C** for 48 hours, respectively. The cell viability is directly related to the absorbance at 490 nm.

9. Cell culture and fluorescent imaging

Cell Culture and Cytotoxicity Assay. MCF7 cells and HeLa cells were purchased at ATCC (Manassas,VA) and were cultured in RPMI 1640 medium (Gibco) and modified Eagle's medium (DMEM, Gibco) in the presence of 10 % fetal bovine serum (FBS, fisher Scientific) under 5 % CO_2 at the temperature, respectively. Standard MTS assay was employed to test the cytotoxicity of rhodamine dyes **A**, **B** and **C** against HeLa cell line. After the cells were further seeded into in a 96-well plate (about 7×10^3 cells per well), and were further incubated for 24 hours. The HeLa cells were put in the fresh culture

medium containing probes **A**, **B**, or **C** with concentration from 0, 5, 10, 15 to 20 μM, and further incubated for 48 h at 37 °C in 5% CO_2 humidified atmosphere, followed by further incubating the cells in a fresh culture medium (80 μL) containing 20 μL CellTiter 96® Aq$_{ueous}$ for another 2 h. Untreated cells were used as controls. The cell viability was determined by making the comparison of the 490 nm absorption between the control cells in the absence of the probe with that of the cells treated with the probe.

Rhodamine dye C applications in cellular Imaging. HeLa cells were seeded into 35 mm x 12 mm glass-bottom culture dishes and incubated for 24 h. When freshly prepared FBS-free medium containing rhodamine dye **C** with concentrations ranging from 1, 5, 10, to 15 μM was used to replace the cell culture medium, the cells was further incubated for 30 min under 5% CO_2 humidified atmosphere. Hoechst and Lysosensor green were added to the solution as the final concentration of 1 μg/ml and 1 μM to incubate another 30 min, respectively. The cells were rinsed with PBS buffer twice again before imaging. To adjust intracellular pH values, the cells were washed with PBS buffer twice before they were treated with 5 μg/mL nigericin in citric buffers with different pH values from 3.0, 3.5, 4.0, 4.5, 5.0, 5.5, 6.0, 6.5, 7.0, 7.5 to equilibrate the intracellular and extracellular pH for 30 min. The cells were incubated with rhodamine dye **C** for 30 min before they were rinsed with PBS buffer twice again for imaging. For the experiment for monitoring lysosomal pH changes, HeLa cells were cultured in medium in the absence and in the presence of 10 mM NH_4Cl, 100 μM NEM (*N*-ethylmaleimide), and 100 μM H_2O_2 before incubating with rhodamine dye **C** for another 30 min. For an experiment under drug stimulation, HeLa cells were cultured in medium in the presence of different concentrations of chloroquine from 50 μM, 100 μM to 200 μM for 30 min followed by incubation with rhodamine dye **C** with another 30 min. Confocal fluorescence microscope (Olympus IX 81) was employed to collect cellular fluorescence images from 425 to 475 nm for blue fluorescence of Hoechst under excitation at 405 nm, from 525 to 575 nm for green fluorescence of Lysosensor green under excitation at 488 nm, and from 650 to 700 nm for red fluorescence of rhodanmine dye **C** under the excitation at 559 nm.

Lysosensor green was used to determine whether rohodamine dye **C** was located in lysosomes in live cells (Figure S37). Confocal microscopic co-localization analysis of rhodamine dye **C** and lysotracker green gave the Pearson's coefficient value of 0.89 or higher, indicating that rhodamine dye **C** accumulates and becomes activated to engender fluorescence in lysosomes in live cells (Figure S37).

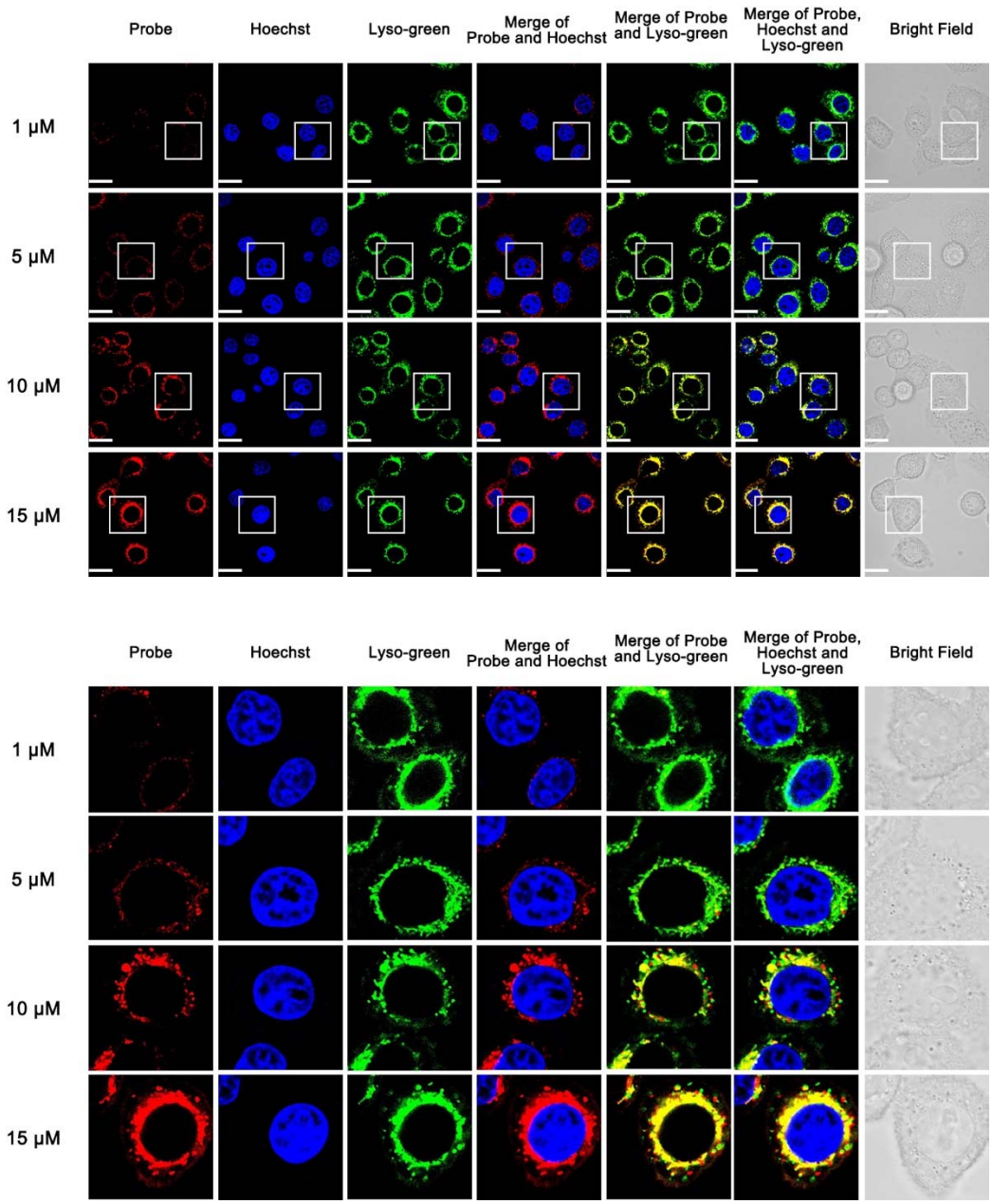

Figure S37. Enlarged acidity-activated turn-on cellular fluorescence images of rhodamine dye **C** in lysosomes in HeLa cells. HeLa cells were cultured in media containing 1 μg/ml Hoechst stain, 1 μM Lysosensor green and rhodamine dye **C** with different concentrations. The images were obtained by confocal fluorescence microscopy with a scale bar of 20 μm.

The filter sets used to image rhodamine dye **C**, Hoechst and Lyso-green were excitation 559 nm and emission 675/50 nm, excitation 405 nm and emission 450/50 nm and excitation 488 nm and emission 550/50 nm, respectively.

We also investigated whether rhodamine dye **C** could be used to detect intracellular pH changes in MCF7 human breast cells. The imaging results convincingly demonstrate that rhodamine dye **C** sensitively responds to intracellular pH changes in MCF7 cells as pH decreases from 7.5 to 4.0 cause cellular fluorescence increases.

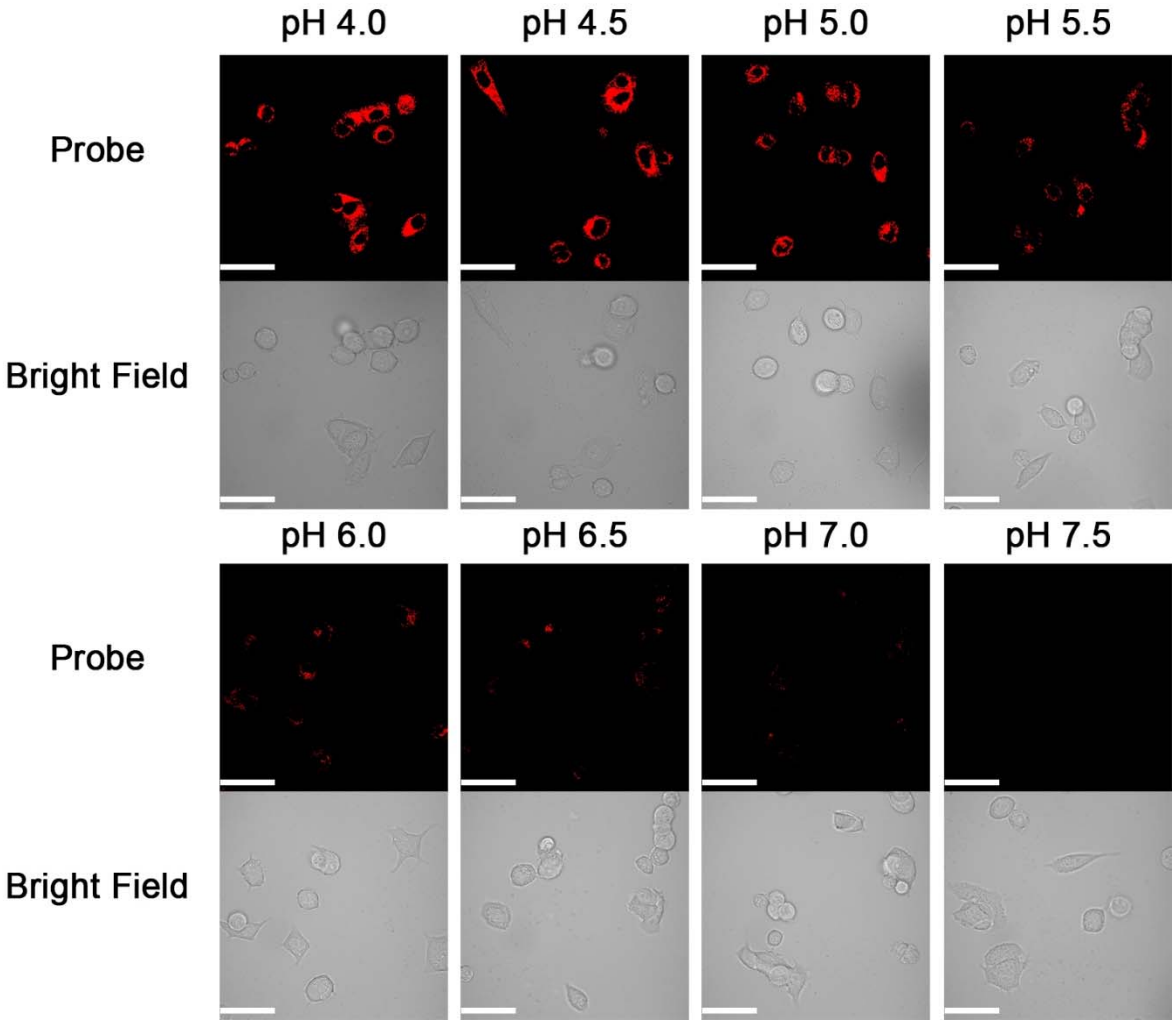

Figure 38. Cellular fluorescence images of 10 μM rhodamine dye **C** inside MCF7 cells with different intracellular pH values, which was adjusted by using 5 μg/mL H^+/K^+ ionophore nigericin to equilibrate the intracellular and extracellular pH in media with different pH values. Confocal fluorescence microscopy was employed to collect the images with a scale bar of 50 μm. The filter sets used to image rhodamine dye **C** was excitation 559 nm and emission 675/50 nm.

10. References

1. T. Jokic, S. M. Borisov, R. Saf, D. A. Nielsen, M. Kuhl and I. Klimant, *Anal. Chem.*, 2012, **84**, 6723-6730.
2. Y. H. Li, Y. J. Wang, S. Yang, Y. R. Zhao, L. Yuan, J. Zheng and R. H. Yang, *Anal. Chem.*, 2015, **87**, 2495-2503.
3. D. D. He, W. Liu, R. Sun, C. Fan, Y. J. Xu and J. F. Ge, *Anal. Chem.*, 2015, **87**, 1499-1502.
4. G. L. Niu, P. P. Zhang, W. M. Liu, M. Q. Wang, H. Y. Zhang, J. S. Wu, L. P. Zhang and P. F. Wang, *Anal. Chem.*, 2017, **89**, 1922-1929.
5. L. Fan, Y. J. Fu, Q. L. Liu, D. T. Lu, C. Dong and S. M. Shuang, *Chem. Commun.*, 2012, **48**, 11202-11204.
6. X. D. Liu, Y. Xu, R. Sun, Y. J. Xu, J. M. Lu and J. F. Ge, *Analyst*, 2013, **138**, 6542-6550.
7. P. Li, H. B. Xiao, Y. F. Cheng, W. Zhang, F. Huang, W. Zhang, H. Wang and B. Tang, *Chem. Commun.*, 2014, **50**, 7184-7187.
8. Q. Q. Wan, S. M. Chen, W. Shi, L. H. Li and H. M. Ma, *Angew. Chem. Int. Ed.*, 2014, **53**, 10916-10920.
9. S. Takahashi, Y. Kagami, K. Hanaoka, T. Terai, T. Komatsu, T. Ueno, M. Uchiyama, I. Koyama-Honda, N. Mizushima, T. Taguchi, H. Arai, T. Nagano and Y. Urano, *J. Am. Chem. Soc.*, 2018, **140**, 5925-5933.
10. T. Myochin, K. Kiyose, K. Hanaoka, H. Kojima, T. Terai and T. Nagano, *J. Am. Chem. Soc.*, 2011, **133**, 3401-3409.
11. J. Y. Zhang, Z. N. Liu, P. Lian, J. Qian, X. W. Li, L. Wang, W. Fu, L. Chen, X. B. Wei and C. Li, *Chem. Sci.*, 2016, **7**, 5995-6005.
12. S. L. Shen, X. F. Zhang, Y. Q. Ge, Y. Zhu, X. Q. Lang and X. Q. Cao, *Sens. Actuator B-Chem.*, 2018, **256**, 261-267.
13. M. X. Fang, S. Xia, J. H. Bi, T. P. Wigstrom, L. Valenzano, J. B. Wang, W. Mazi, M. Tanasova, F. T. Luo and H. Y. Liu, *Chem. Commun.*, 2018, **54**, 1133-1136.
14. X. F. Zhang, C. Wang, Z. Han and Y. Xiao, *Acs Appl. Mater. Interfaces*, 2014, **6**, 21669-21676.
15. J. B. Wang, S. Xia, J. H. Bi, M. X. Fang, W. F. Mazi, Y. B. Zhang, N. Conner, F. T. Luo, H. P. Lu and H. Y. Liu, *Bioconjug. Chem.*, 2018, **29**, 1406-1418.
16. S. W. Zhang, T. H. Chen, H. M. Lee, J. H. Bi, A. Ghosh, M. X. Fang, Z. C. Qian, F. Xie, J. Ainsley, C. Christov, F. T. Luo, F. Zhao and H. Y. Liu, *ACS Sens.*, 2017, **2**, 924-931.
17. J. T. Zhang, M. Yang, W. F. Mazi, K. Adhikari, M. X. Fang, F. Xie, L. Valenzano, A. Tiwari, F. T. Luo and H. Y. Liu, *ACS Sens.*, 2016, **1**, 158-165.
18. J. T. Zhang, M. Yang, C. Li, N. Dorh, F. Xie, F. T. Luo, A. Tiwari and H. Y. Liu, *J. Mater. Chem. B*, 2015, **3**, 2173-2184.
19. S. Xia, J. B. Wang, J. H. Bi, X. Wang, M. X. Fang, T. Phillips, A. May, N. Conner, M. Tanasova, F. T. Luo and H. Y. Liu, *Sens. Actuator B-Chem.*, 2018, **265**, 699-708.
20. W. Chen, S. Xu, J. J. Day, D. Wang and M. Xian, *Angew. Chem.*, 2017, **129**, 16838-16842.
21. S. Kamino, M. Murakami, M. Tanioka, Y. Shirasaki, K. Watanabe, J. Horigome, Y. Ooyama and S. Enomoto, *Organic Letters*, 2014, **16**, 258-261.
22. Y.-J. Gong, X.-B. Zhang, G.-J. Mao, L. Su, H.-M. Meng, W. Tan, S. Feng and G. Zhang, *Chemical Science*, 2016, **7**, 2275-2285.
23. Y. Yuan, S. Xu, X. Cheng, X. Cai and B. Liu, *Angew. Chem. Int. Ed. Engl.*, 2016, **55**, 6457-6461.
24. L. Yuan, W. Lin, Y. Yang and H. Chen, *J. Am. Chem.Soc.*, 2012, **134**, 1200-1211.
25. E. Cielen, A. Tahri, K. Ver Heyen, G. J. Hoornaert, F. C. De Schryver and N. Boens, *Journal of the Chemical Society, Perkin Transactions 2*, 1998, DOI: 10.1039/A802183J, 1573-1580.
26. S. Melchor and J. A. Dobado, *J. Chem. Inf. Comput. Sci.*, 2004, **44**, 1639-1646.

27. M. D. Hanwell, D. E. Curtis, D. C. Lonie, T. Vandermeersch, E. Zurek and G. R. Hutchison, *Journal of Cheminformatics*, 2012, **4**, 17.
28. GaussView, V. 6, R. Dennington, T. A. Keith and J. M. Millam, Semichem Inc. Shawnee Mission, KS, 2016.
29. A. Austin, G. A. Petersson, M. J. Frisch, F. J. Dobek, G. Scalmani and K. Throssell, *Journal of Chemical Theory and Computation*, 2012, **8**, 4989-5007.
30. K. Raghavachari and G. W. Trucks, *J. Chem. Phys.*, 1989, **91**, 1062-1065.
31. A. J. H. Wachters, *J. Chem. Phys.*, 1970, **52**, 1033-1036.
32. P. J. Hay, *J. Chem. Phys.*, 1977, **66**, 4377-4384.
33. Gaussian 16 Revision A.03, M. J. Frisch, G. W. Trucks, H. B. Schlegel, G. E. Scuseria, M. A. Robb, J. R. Cheeseman, G. Scalmani, V. Barone, G. A. Petersson, H. Nakatsuji, X. Li, M. Caricato, A. V. Marenich, J. Bloino, B. G. Janesko, R. Gomperts, B. Mennucci, H. P. Hratchian, J. V. Ortiz, A. F. Izmaylov, J. L. Sonnenberg, Williams, F. Ding, F. Lipparini, F. Egidi, J. Goings, B. Peng, A. Petrone, T. Henderson, D. Ranasinghe, V. G. Zakrzewski, J. Gao, N. Rega, G. Zheng, W. Liang, M. Hada, M. Ehara, K. Toyota, R. Fukuda, J. Hasegawa, M. Ishida, T. Nakajima, Y. Honda, O. Kitao, H. Nakai, T. Vreven, K. Throssell, J. A. Montgomery Jr., J. E. Peralta, F. Ogliaro, M. J. Bearpark, J. J. Heyd, E. N. Brothers, K. N. Kudin, V. N. Staroverov, T. A. Keith, R. Kobayashi, J. Normand, K. Raghavachari, A. P. Rendell, J. C. Burant, S. S. Iyengar, J. Tomasi, M. Cossi, J. M. Millam, M. Klene, C. Adamo, R. Cammi, J. W. Ochterski, R. L. Martin, K. Morokuma, O. Farkas, J. B. Foresman and D. J. Fox, *Journal*, 2016.
34. M. E. Casida, C. Jamorski, K. C. Casida and D. R. Salahub, *J. Chem. Phys.*, 1998, **108**, 4439-4449.
35. E. Cancès, B. Mennucci and J. Tomasi, *J. Chem. Phys.*, 1997, **107**, 3032-3041.
36. L. Skripnikov, *Chemissian*, 2005-2017, **www.chemissian.com**.